

An Imprecise SHAP as a Tool for Explaining the Class Probability Distributions under Limited Training Data

Lev V. Utkin, Andrei V. Konstantinov, and Kirill A. Vishniakov
 Peter the Great St.Petersburg Polytechnic University
 St.Petersburg, Russia

e-mail: lev.utkin@gmail.com, andrue.konst@gmail.com, ki.vishniakov@gmail.com

Abstract

One of the most popular methods of the machine learning prediction explanation is the SHapley Additive exPlanations method (SHAP). An imprecise SHAP as a modification of the original SHAP is proposed for cases when the class probability distributions are imprecise and represented by sets of distributions. The first idea behind the imprecise SHAP is a new approach for computing the marginal contribution of a feature, which fulfils the important efficiency property of Shapley values. The second idea is an attempt to consider a general approach to calculating and reducing interval-valued Shapley values, which is similar to the idea of reachable probability intervals in the imprecise probability theory. A simple special implementation of the general approach in the form of linear optimization problems is proposed, which is based on using the Kolmogorov-Smirnov distance and imprecise contamination models. Numerical examples with synthetic and real data illustrate the imprecise SHAP.

Keywords: interpretable model, XAI, Shapley values, SHAP, Kolmogorov-Smirnov distance, imprecise probability theory.

1 Introduction

An importance of the machine learning models in many applications and their success in solving many applied problems lead to another problem which may be an obstacle for using the models in areas where their prediction accuracy as well as understanding is crucial, for example, in medicine, reliability analysis, security, etc. This obstacle takes place for complex models which can be viewed as black boxes because their users do not know how the models act and are functioning. Moreover, the training process is also often unknown. A natural way for overcoming the obstacle is to use a meta-model which could explain the provided predictions. The explanation means that we have to select features of an analyzed example which are responsible for the prediction of the obtained black-box model or significantly impact on the corresponding prediction. By considering the explanation of a single example, we say about the

so-called local explanation methods. They aim to explain the black-box model locally around the considered example. Another explanation methods try to explain predictions taking into account the whole dataset or its certain part. The need of explaining the black-box models using the local or global explanations in many applications motivated developing a huge number of explanation methods which are described in detail in several comprehensive survey papers [10, 29, 41, 47, 49, 68, 79, 82, 85].

Among all explanation methods, we select two very popular methods: the Local Interpretable Model-Agnostic Explanation (LIME) [60] and SHapley Additive exPlanations (SHAP) [44, 72]. The basic idea behind LIME is to build an approximating linear model around the explained example. In order to implement the approximation, many synthetic examples are generated in the neighborhood of the explained example with weights depending on distances from the explained example. The linear regression model is constructed by using the generated examples such that its coefficients can be regarded as quantitative representation of impacts of the corresponding features on the prediction.

SHAP is inspired by game-theoretic Shapley values [71] which can be interpreted as average expected marginal contributions over all possible subsets (coalitions) of features to the black-box model prediction. In spite of two important shortcomings of SHAP, including its computational complexity depending on the number of features and some ambiguity of available approaches for removing features from consideration [17], SHAP is widely used in practice and can be viewed as the most promising and theoretically justified explanation method which fulfils several nice properties [44]. Nevertheless, another difficulty of using SHAP is how to deal with predictions in the form of probability distributions which arise in multi-class classification and in machine learning survival analysis. The problem is that SHAP in each iteration calculates a difference between two predictions defined by different subsets of features in the explained example. Therefore, the question is how to define the difference between the probability distributions. One of the simplest ways in classification is to consider a class with the largest probability. However, this way may lead to incorrect results when the probabilities are comparable. Moreover, the same approach cannot be applied to explanation of the survival model predictions which are in the form of survival functions. It should be noted that Covert et al. [18] justified that the well-known Kullback-Leibler (KL) divergence [40] can be applied to the global explanation. It is obvious that the KL divergence can be applied also to the local explanation. Moreover, the KL divergence can be replaced with different distances, for example, χ^2 -divergence [56], the relative J-divergence [23], Csiszar's f -divergence measure [19]. However, the use of all these measures leads to such modifications of SHAP that obtained Shapley values do not satisfy properties of original Shapley values. Therefore, one of the problems for solving is to define a meaningful distance between two predictions represented in the form of the class probability distributions, which fulfils the Shapley value properties.

It should be noted that the probability distribution of classes may be imprecise due to a limited number of training data. On the one hand, it can be said that the class probabilities in many cases are not real probabilities as measures defined on events, i.e., they are not relative frequencies of occurrence of events. For example, the softmax function in neural networks produce numbers (weights of classes), which have some properties of probabilities, but not original probabilities. On the other hand, probabilities of classes in random forests and in random sur-

vival forests can be viewed as relative frequencies (probabilities are computed by counting the percentage of different classes of examples at each leaf node), and they are true probabilities. In both the cases, it is obvious that accuracy of the class probability distributions depends on the machine learning model predicting the distributions and on the amount of training data. It is difficult to impact on improvement of the post-hoc machine learning model representing as a black box, but we can take into account the imprecision of probability distributions due to the lack of sufficient training data.

The considered imprecision can be referred to the epistemic uncertainty [69] which represents our ignorance about a model caused by the lack of observation data. Epistemic uncertainty can be resolved by observing more data. There are several approaches to formalize the imprecision. One of them is to consider a set of probability distributions instead of the single one. Sets of distributions are produced by imprecise statistical models, for example, by the linear-vacuous mixture or imprecise ε -contamination model [76], by the imprecise Dirichlet model [77], by the constant odds-ratio model [76], by Kolmogorov–Smirnov bounds [34]. It is obvious that the above imprecise statistical models produce interval-valued probabilities of events or classes, and the obtained interval can be regarded as a measure of observation data insufficiency.

It turns out that the imprecision of the class probability distribution leads to imprecision of Shapley values when SHAP is used for explaining the machine learning model predictions. In other words, Shapley values become interval-valued. This allows us to construct a new framework of the imprecise SHAP or imprecise Shapley values, which provides a real accounting of the prediction uncertainty. Having the interval-valued Shapley values, we can compare intervals in order to select the most important features. It is interesting to point out that properties of the efficiency and the linearity of Shapley values play a crucial role in constructing basic rules of the framework of imprecise Shapley values.

In summary, the following contributions are made in this paper:

1. A new approach for computing the marginal contribution of the i -th feature in SHAP for interpretation of the class probability distributions as predictions of a black-box machine learning model is proposed. It is based on considering a distance between two probability distributions. Moreover, Shapley values using the proposed approach fulfils the efficiency property which is very important in correct explanation by means of SHAP.
2. An imprecise SHAP is proposed for cases when the class probability distributions are imprecise, i.e., they are represented by convex sets of distributions. The outcome of the imprecise SHAP is a set of interval-valued Shapley values. Basic tools for dealing with imprecise class probability distributions and for computing interval-valued Shapley values are introduced.
3. Implementation of the imprecise SHAP by using the Kolmogorov-Smirnov distance is proposed. Complex optimization problems for computing interval-valued Shapley values are reduced to finite sets of simple linear programming problems.
4. The imprecise SHAP is illustrated by means of numerical experiments with synthetic and real data.

The code of the proposed algorithm can be found in <https://github.com/LightnessOfBeing/ImpreciseSHAP>

The paper is organized as follows. Related work is in Section 2. A brief introduction to Shapley values and SHAP itself is given in Section 3 (Background). A new approach for

computing the marginal contribution of each feature in SHAP for multiclassification problems is provided in Section 4. The imprecise SHAP is introduced in Section 5. Application of the Kolmogorov-Smirnov distance to the imprecise SHAP to get simple calculations of the interval-valued Shapley values is considered in Section 6. Numerical experiments with synthetic data and real data are given in Section 7. Concluding remarks can be found in Section 8.

2 Related work

Local interpretation methods. An increasing importance of machine learning models and algorithms leads to development of new explanation methods taking into account various peculiarities of applied problems. As a result, many models of the local interpretation has been proposed. Success and simplicity of LIME resulted in development of several its modifications, for example, ALIME [70], Anchor LIME [61], LIME-Aleph [58], GraphLIME [31], SurvLIME [39], etc. A comprehensive analysis of LIME, including the study of its applicability to different data types, for example, text and image data, is provided by Garreau and Luxburg [27]. The same analysis for tabular data is proposed by Garreau and Luxburg [28]. An image version of LIME with its thorough theoretical investigation is presented by Garreau and Mardaoui [26]. An interesting information-theoretic justification of interpretation methods on the basis of the concept of explainable empirical risk minimization is proposed by Jung [35].

In order to relax the linearity condition for the local interpretation models like LIME and to adequately approximate a black-box model, several methods based on using Generalized Additive Models (GAMs) [30] were proposed [16, 43, 54, 84]. Another interesting class of models based on using a linear combination of neural networks such that a single feature is fed to each network was proposed by Agarwal et al. [7]. The impact of every feature on the prediction in these models is determined by its corresponding shape function obtained by each neural network. Following ideas behind these interpretation models, Konstantinov and Utkin [37] proposed a similar model, but an ensemble of gradient boosting machine is used instead of neural networks in order to simplify the explanation model training process.

Another explanation method is SHAP [44, 72], which takes a game-theoretic approach for optimizing a regression loss function based on Shapley values. General questions of the computational efficiency of SHAP were investigated by Van den Broeck et al. [21]. Bowen and Ungar [14] proposed the generalized SHAP method (G-SHAP) which allows us to compute the feature importance of any function of a model’s output. Rozemberczki and Sarkar [64] presented an approach to applying SHAP to ensemble models. The problem of explaining the predictions of graph neural networks by using SHAP was considered by Yuan et al. [81]. Frye et al. [25] introduced the so-called off- and on-manifold Shapley values for high-dimensional multi-type data. Application of SHAP to explanation of recurrent neural networks was studied in [12]. Begley et al. present a new approach to explaining fairness in machine learning, based on the Shapley value paradigm. Antwarg et al. [8] studied how to explain anomalies detected by autoencoders using SHAP. The problem of explaining anomalies detected by PCA is also considered by Takeishi [73]. SHAP is also applied to problems of explaining individual predictions when features are dependent [1] or when features are mixed [59]. SHAP has been

used in real applications to explain predictions of the black-box models, for example, it was used to rank failure modes of reinforced concrete columns and to explain why a machine learning model predicts a specific failure mode for a given sample [45]. It was also used in chemoinformatics and medicinal chemistry [63].

A lot of interpretation methods, their analysis, and critical review can be found also in survey papers [6, 9, 10, 15, 20, 29, 41, 67, 79].

Imprecise probabilities in classification and regression. One of the first ideas of applying imprecise probability theory to classification decision trees was presented in [5], where probabilities of classes at decision tree leaves are estimated by using an imprecise model, and the so-called Credal Decision Tree model is proposed. Following this work, several papers devoted to applications of imprecise probabilities to decision trees and random forests were presented [3, 4, 46, 52], where the authors developed new splitting criteria taking into account imprecision of training data and noisy data. In particular, the authors consider the application of Walley’s imprecise Dirichlet model (IDM) [77]. The main advantage of the IDM in its application to the classification problems is that it produces a convex set of probability distributions, which has nice properties and depends on a number of observations. Another interesting model called the fuzzy random forest is proposed in [13]. As an alternative to the use of the IDM, nonparametric predictive inference has also been used successfully for imprecise probabilistic inference with decision trees [2]. Imprecise probabilities have also been used in classification problems in [22, 48, 51]. The main focus of interest in this paper is not imprecise probabilities in machine learning models, but imprecision of Shapley values as a consequence of the machine learning model prediction imprecision when SHAP is used to explain the model prediction.

3 Shapley values and model explainability

One of the approaches to explaining machine learning model predictions is the Shapley value [71] as a concept in coalitional games. According to the concept, the total gain of a game is distributed among players such that desirable properties, including efficiency, symmetry, and linearity, are fulfilled. In the framework of the machine learning, the gain can be viewed as the machine learning model prediction or the model output, and a player is a feature of input data. Hence, contributions of features to the model prediction can be estimated by Shapley values. The i -th feature importance is defined by the Shapley value

$$\phi_i(f) = \phi_i = \sum_{S \subseteq N \setminus \{i\}} B(S, N) [f(S \cup \{i\}) - f(S)], \quad (1)$$

where $f(S)$ is the black-box model prediction under condition that a subset S of features are used as the corresponding input; N is the set of all features; $B(S, N)$ is defined as

$$B(S, N) = \frac{|S|! (|N| - |S| - 1)!}{|N|!}. \quad (2)$$

It can be seen from (1) that the Shapley value ϕ_i can be regarded as the average contribution of the i -th feature across all possible permutations of the feature set.

The Shapley value has the following well-known properties:

Efficiency. The total gain is distributed as $\sum_{k=0}^m \phi_k = f(\mathbf{x}) - f(\emptyset)$.

Symmetry. If two players with numbers i and j make equal contributions, i.e., $f(S \cup \{i\}) = f(S \cup \{j\})$ for all subsets S which contain neither i nor j , then $\phi_i = \phi_j$.

Dummy. If a player makes zero contribution, i.e., $f(S \cup \{j\}) = f(S)$ for a player j and all $S \subseteq N \setminus \{j\}$, then $\phi_j = 0$.

Linearity. A linear combination of multiple games f_1, \dots, f_n , represented as $f(S) = \sum_{k=1}^n c_k f_k(S)$, has gains derived from f : $\phi_i(f) = \sum_{k=1}^n c_k \phi_i(f_k)$ for every i .

Let us consider a machine learning problem. Suppose that there is a dataset $\{(\mathbf{x}_1, y_1), \dots, (\mathbf{x}_n, y_n)\}$ of n points (\mathbf{x}_i, y_i) , where $\mathbf{x}_i \in \mathcal{X} \subset \mathbb{R}^m$ is a feature vector consisting of m features, y_i is the observed output for the feature vector \mathbf{x}_i such that $y_i \in \mathbb{R}$ in the regression problem and $y_i \in \{1, 2, \dots, T\}$ in the classification problem with T classes.

If the task is to interpret or to explain prediction $f(\mathbf{x}^*)$ from the model at a local feature vector \mathbf{x}^* , then the prediction $f(\mathbf{x}^*)$ can be represented by using Shapley values as follows [44, 72]:

$$f(\mathbf{x}^*) = \phi_0 + \sum_{j=1}^m \phi_j^*, \quad (3)$$

where $\phi_0 = \mathbb{E}[f(\mathbf{x})]$, ϕ_j^* is the value ϕ_j for the prediction $\mathbf{x} = \mathbf{x}^*$.

The above implies that Shapley values explain the difference between prediction $f(\mathbf{x}^*)$ and the global average prediction.

One of the crucial questions for implementing SHAP is how to remove features from subset $N \setminus S$, i.e., how to fill input features from subset $N \setminus S$ in order to get predictions $f(S)$ of the black-box model. A detailed list of various ways for removing features is presented by Covert et al. [17]. One of the ways is simply by setting the removed features to zero [57, 83] or by setting them to user-defined default values [60]. According to the way, features are often replaced with their mean values. Another way removes features by replacing them with a sample from a conditional generative model [80]. In the LIME method for tabular data, features are replaced with independent draws from specific distributions [17] such that each distribution depends on original feature values. These are only a part of all ways for removing features.

4 SHAP and multiclassification problems

4.1 SHAP and the Kullback-Leibler divergenc

Let us consider a classification model f whose predictions for the subset $S \cup \{i\}$ are probabilities p_1, \dots, p_C of C classes under conditions $p_1 + \dots + p_C = 1$ and $p_k \geq 0$ for all k . The probabilities can be regarded as a distribution $P(S) = (p_1, \dots, p_C)$ over a C -class categorical variable. Suppose that the prediction of the model f for the subset S is a distribution denoted as $Q(S) = (q_1, \dots, q_C)$, where $q_1 + \dots + q_C = 1$ and $q_k \geq 0$ for all k .

Covert et al. [18] justified that the Kullback-Leibler divergence $KL(P||Q)$ is a natural way to measure the deviation of the predictions from P and Q for the global explanation.

Indeed, this is a very interesting idea to consider the KL divergence instead of the difference $f(S \cup \{i\}) - f(S)$. Lower the KL divergence value, the better we have matched the true distribution with our approximation, and the smaller we have impact of the i -th feature. Then (1) can be rewritten as

$$\phi_i(f) = \phi_i = \sum_{S \subseteq N \setminus \{i\}} B(S, N) KL(P(S) || Q(S)). \quad (4)$$

Let us return to some properties of the Kullback-Leibler divergence. First, it is assumed that either $q_i \neq 0$ for all values of i , or that if one $p_i = 0$, then $q_i = 0$ as well. In this case, there holds $0/0 = 1$. Second, it is called the information gain achieved if P would be used instead of Q which is currently used. In Bayesian interpretation, the KL divergence shows updating from a prior distribution Q (without knowledge the i -th feature) to the posterior distribution P (with the available i -th feature). Third, the KL divergence is a non-symmetric measure. This idea has a deeper meaning. It means that generally $KL(P||Q) \neq KL(Q||P)$. The last property is very important. Indeed, when we say that the i -th feature positively contributes into the prediction for some S , this means that $f(S \cup \{i\}) - f(S) > 0$ and does not mean that $f(S) - f(S \cup \{i\}) > 0$, i.e., the contribution is also non-symmetric to some extent. This implies that the replacement of the difference $f(S \cup \{i\}) - f(S)$ with measure KL should fulfil the following property: $KL(P||Q) \geq KL(Q||P)$ if the i -th feature positively contributes into the prediction. This also means that we cannot use one of the standard symmetric distance metrics for getting the difference between predictions. It should distinguish here the symmetry property of the divergence measure and the symmetry property of the Shapley values.

4.2 Interpretation of the predicted distribution P_S

Suppose that the black-box classification model provides a class probability distribution $P_N = f(N)$ as its prediction for the input data with features from the set N . Without loss of generality, we assume that P_N is close to the vector $(1, 0, \dots, 0)$. In order to use the SHAP, we have to consider two types of probability distributions: $P_{S \cup i} = f(S \cup \{i\})$ and $P_S = f(S)$, where $S \subseteq N \setminus \{i\}$ (see (1)).

Let us define a function of predictions P_S as well as $P_{S,i}$ for all S and i as the distance between P_N and P_S or P_N and $P_{S \cup i}$, denoted as $D(P_S, P_N)$ or $D(P_{S,i}, P_N)$, respectively. Let us also introduce the marginal contribution of the i -th feature as $D(P_S, P_N) - D(P_{S,i}, P_N)$. This is an unusual definition of the marginal contribution can be explained by means of Fig. 1 where two cases of the predicted probability distributions of examples having three features are illustrated in the probabilistic unit simplex with vertices $(1, 0, 0)$, $(0, 1, 0)$, $(0, 0, 1)$. Distributions $P_{S \cup i}$ and P_S are depicted by small triangles. Distribution P_N is depicted by the small circle.

At first glance, it seems that the contribution of the i -th feature should be measured by the distance between points P_S and $P_{S,i}$. In particular, if the points coincide, then the distance is zero, and there is no contribution of the considered feature into the prediction or into the class probability distribution. Moreover, Covert et al. [18] proposed to apply the KL divergence $KL(P_{S,i} || P_S)$ to characterize the feature marginal contribution. However, if we look at the

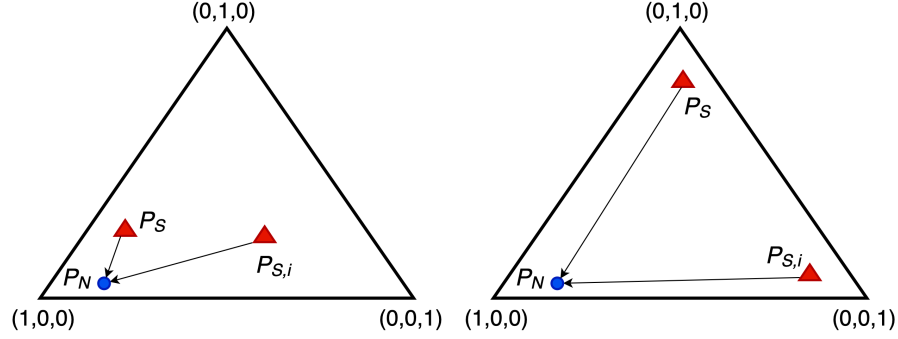


Figure 1: Two cases of the relationship between probability distributions P_N , P_S , $P_{S,i}$

right unit simplex in Fig. 1, then we can see that the distance between P_S and $P_{S,i}$ is very large. Hence, the marginal contribution of the i -th feature should be large. However, after adding the i -th feature, we remain to be at the same distance from P_N . We do not improve our knowledge about the true class or about P_N after adding the i -th feature to S and computing the corresponding prediction. Note that we do not search for the contribution of the i -th feature into the prediction P_S . We aim to estimate how the i -th feature contributes into P_N . Points P_S and $P_{S,i}$ in the right simplex are approximately at the same distance from P_N , therefore, the difference $D(P_S, P_N) - D(P_{S,i}, P_N)$ is close to 0 though points P_S and $P_{S,i}$ are far from each other. The left unit simplex in Fig. 1 shows a different case when $P_{S,i}$ negatively contributes into our knowledge about the class distribution P_N because it makes the probability distribution to be more uncertain in comparison with P_S . This implies that the difference $D(P_S, P_N) - D(P_{S,i}, P_N)$ should be negative in this case.

Assuming that $D(P_S, P_N)$ is the KL divergence, this distance can be regarded as the information gain achieved if P_S would be used instead of P_N . A similar information gain is achieved if $P_{S,i}$ would be used instead of P_N . Then we can conclude that the difference $D(P_S, P_N) - D(P_{S,i}, P_N)$ can be regarded as the contribution of the i -th feature in the change of information gain.

The problem arises when we consider a case illustrated in Fig. 2, where points P_S and $P_{S,i}$ are at the same distance from P_N . However, this case can be also explained in the same way. We do not interpret a final decision about a class of the example. The distribution P_0 is interpreted here. But this distribution is correctly interpreted because the distribution $P_{S,i}$ does not contribute into P_N in comparison with the distribution P_S . The distribution P_S explains the decision (1,0,0) better than $P_{S,i}$, but not than P_N . Here we meet a situation when interpretation strongly depends on its aim. If its aim is to interpret P_N without taking into account the final decision about a class, then we should use the above approach, and contribution of the i -th feature in the case illustrated in Fig. 2 is 0.

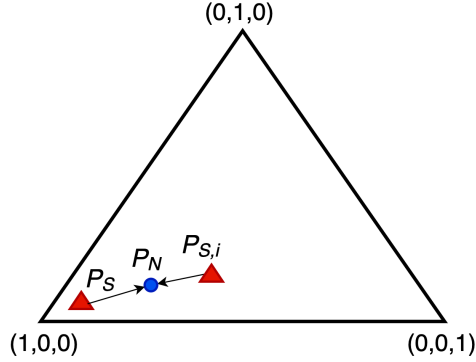


Figure 2: A specific case of the probability distribution location

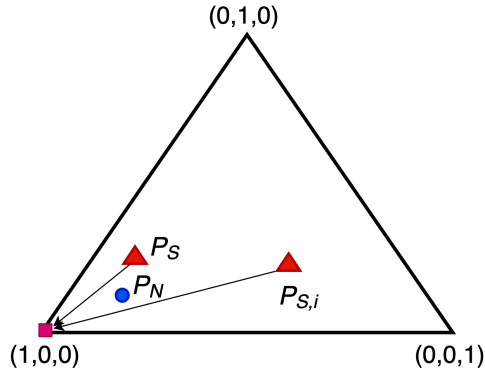


Figure 3: Interpretation of the predicted class

4.3 Interpretation of the predicted class

Another case is when our aim is to explain the final decision about the predicted class by having predictions in the form of probability distributions. The class can be represented by the probability distribution $P_0 = (1, 0, \dots, 0)$ which is depicted in Fig. 3 by a small square. In this case, we compare distributions P_S and $P_{S,i}$ with P_0 , but not with P_N because we analyze how the i -th feature contributes into change of the decision about the class of the corresponding example, or how this feature contributes into our knowledge about the true class. This is an important difference from the above case when we interpreted P_N . It can be seen from Fig. 3 that we compute distances $D(P_S, P_0)$ and $D(P_{S,i}, P_0)$ instead of $D(P_S, P_N)$ and $D(P_{S,i}, P_N)$, respectively. When interpretation of the class is performed, the contribution of the i -th feature for the case shown in Fig. 2 is no longer zero. Therefore, we will distinguish the above two cases: interpretation of the class probability distribution and interpretation of the predicted class by using the predicted class probability distribution.

It seems that the distance $D(P_S, P_0)$ could be viewed as a measure of uncertainty of the prediction P_S . However, if we assume that $P_0 = (1, 0, 0)$ and $P_S = (0, 1, 0)$, then the distance

between distributions is largest, but the distribution P_S is certain. In order to consider the uncertainty measure, the distance $D(P_S, P_u)$ should be studied in place of $D(P_S, P_0)$, where P_u is the uniform distribution $(1/C, \dots, 1/C)$. In this case, the distance $D(P_S, P_u)$ is a certainty measure of P_S , because the most uncertain case when $P_S = P_u$ leads to $D(P_S, P_u) = 0$.

4.4 Properties of Shapley values and the introduced distances

In sum, the Shapley values are computed now as follows:

$$\phi_i = \sum_{S \subseteq N \setminus \{i\}} B(S, N) [D(P_S, P_N) - D(P_{S,i}, P_N)]. \quad (5)$$

Let us study how the introduced distances fulfil basic properties of Shapley values. Their proof directly follows from the representation of the prediction $f(S)$ as $-D(P_S, P_N)$ or $-D(P_S, P_0)$. Since the condition $f(\emptyset) = 0$ may be not valid (the prediction by some predefined feature values), then the efficiency property is rewritten as follows. For the case of the interpretation of the predicted distribution P_S , the total gain is determined as

$$\begin{aligned} \sum_{k=1}^m \phi_k &= f(\mathbf{x}) - f(\emptyset) = -D(P_N, P_N) + D(P_\emptyset, P_N) \\ &= D(P_\emptyset, P_N). \end{aligned} \quad (6)$$

Here P_\emptyset is the black-box model prediction by replacing all features with some predefined values, for example, with mean values.

Other properties of the Shapley values, including the symmetry, dummy and linearity properties, remain without changes.

5 Imprecise extension of SHAP

5.1 SHAP by sets of probability distributions (a general approach)

We assume that a prediction of the black-box model is imprecise due to a small amount of training data, due to our ignorance about a model caused by the lack of observation data. In order to take into account the imprecision, it is proposed to replace precise probability distributions of classes by sets of probability distributions denoted as \mathcal{P} , which can be constructed in accordance with one of the well-known imprecise statistical inference models [76].

The imprecision of predictions changes the definition of distances between probability distributions because precise distributions are replaced with sets of probability distributions \mathcal{P} . This implies that distances between sets \mathcal{P}_1 and \mathcal{P}_2 of distributions should be defined instead of distances between single distributions. We have now a set of distances between all pairs of points such that one point in each pair belongs to set \mathcal{P}_1 , and another point in the pair belongs to set \mathcal{P}_2 . As a result, the set of distances produces an interval with some lower and upper bounds corresponding to the smallest and the largest distances, respectively. The same can

be said about pairs of distributions which produce an interval of Shapley values ϕ_i denoted as $[\phi_i^L, \phi_i^U]$. This implies that (5) can be rewritten as

$$\phi_i^L = \sum_{S \subseteq N \setminus \{i\}} B(S, N) \min_{P \in \mathcal{P}(P_S), R \in \mathcal{P}(P_{S,i}), Q \in \mathcal{P}(P_N)} [D(P, Q) - D(R, Q)], \quad (7)$$

$$\phi_i^U = \sum_{S \subseteq N \setminus \{i\}} B(S, N) \max_{P \in \mathcal{P}(P_S), R \in \mathcal{P}(P_{S,i}), Q \in \mathcal{P}(P_N)} [D(P, Q) - D(R, Q)], \quad (8)$$

where P, R, Q are probability distributions from subsets $\mathcal{P}(P_S), \mathcal{P}(P_{S,i}), \mathcal{P}(P_N)$, respectively.

We do not define strongly subsets $\mathcal{P}(P_S), \mathcal{P}(P_{S,i}), \mathcal{P}(P_N)$ in order to derive general results. We only assume that every subset is convex and is a part of the unit simplex of probabilities. Specific imprecise statistical models producing sets of probability distributions will be considered below.

The next question is how to calculate intervals for Shapley values. A simple way is to separately compute the minimum and the maximum of distances D , namely, as follows:

$$\phi_i^L = \sum_{S \subseteq N \setminus \{i\}} B(S, N) \left[\min_{P \in \mathcal{P}(P_S), Q \in \mathcal{P}(P_N)} D(P, Q) - \max_{R \in \mathcal{P}(P_{S,i}), Q \in \mathcal{P}(P_N)} D(R, Q) \right], \quad (9)$$

$$\phi_i^U = \sum_{S \subseteq N \setminus \{i\}} B(S, N) \left[\max_{P \in \mathcal{P}(P_S), Q \in \mathcal{P}(P_N)} D(P, Q) - \min_{R \in \mathcal{P}(P_{S,i}), Q \in \mathcal{P}(P_N)} D(R, Q) \right], \quad (10)$$

However, obtained intervals of Shapley values may be too wide because we actually consider extreme cases assuming that the distribution $Q \in \mathcal{P}(P_N)$ may be different in different distances, i.e., in $D(P, Q)$ and $D(R, Q)$. This assumption might be reasonable. Moreover, it would significantly simplify the optimization problems. In order to obtain tighter intervals, we return to (7)-(8). We assume that there exists a single class probability distribution Q from $\mathcal{P}(P_N)$, which is unknown, but it provides the smallest or the largest value of $D(P, Q) - D(R, Q)$ over all distributions from $\mathcal{P}(P_N)$. Of course, we relax this condition in other terms of the sum over $S \subseteq N \setminus \{i\}$ because it is extremely difficult to solve the obtained optimization problem under this condition. The same can be said about distributions P and R . As a result, we also get wide intervals for Shapley values because, but they will be reduced taking into account intervals for all Shapley values and the efficiency property of the values.

Solutions of optimization problems in (7) and (8) depend on definitions of the distance D . Let us return to the efficiency property (6) which is briefly written as $\sum_{k=0}^m \phi_k = D(P_\emptyset, P_N)$. Suppose that we have computed ϕ_i^L and ϕ_i^U . Let us denote the lower and upper bounds for $D(P_\emptyset, P_N)$ as D^L and D^U , respectively. Then there hold

$$D^L = \min_{T \in \mathcal{P}(P_\emptyset), Q \in \mathcal{P}(P_N)} D(T, Q), \quad (11)$$

$$D^U = \max_{T \in \mathcal{P}(P_\emptyset), Q \in \mathcal{P}(P_N)} D(T, Q). \quad (12)$$

Hence, the efficiency property of Shapley values can be rewritten by taking into account interval-valued Shapley values as

$$D^L \leq \sum_{k=1}^m \phi_k \leq D^U. \quad (13)$$

It follows from (13) that we cannot write a precise version of the efficiency property because we do not know precise distributions P_\emptyset and P_N . Therefore, we use bounds for the total gain, but these bounds can help us to reduce intervals of ϕ_i . Reduced intervals can be obtained by solving the following linear optimization problems:

$$\tilde{\phi}_k^L = \min \phi_k, \quad \tilde{\phi}_k^U = \max \phi_k, \quad (14)$$

subject to (13) and $\phi_k^L \leq \phi_k \leq \phi_k^U$, $k = 1, \dots, m$.

The above optimization problems for all k from 1 to m allow us to get tighter bounds for Shapley values. It turns out that problems (14) can be explicitly solved. In order to avoid introducing new notations, we assume that all Shapley values are positive. It can be done by subtracting value $\min_{i=1, \dots, m} \phi_i^L$ from all variables ϕ_i .

Proposition 1 *Assume that $\min_{i=1, \dots, m} \phi_i^L \geq 0$ and*

$$\sum_{i=1}^m \phi_i^L \leq D^L, \quad \sum_{i=1}^m \phi_i^U \geq D^U. \quad (15)$$

Then problems (14) have the following solutions for all $k \in \{1, \dots, m\}$:

$$\tilde{\phi}_k^U = \min \left(\phi_k^U, D^U - \sum_{i=1, i \neq k}^m \phi_i^L \right), \quad (16)$$

$$\tilde{\phi}_k^L = \max \left(\phi_k^L, D^L - \sum_{i=1, i \neq k}^m \phi_i^U \right). \quad (17)$$

It is interesting to note that the above problem statement is similar to the definitions of reachable probability intervals [22] in the framework of the imprecise probability theory [76]. It can be regarded as an extension of the probabilistic definitions which consider sets of probability distributions as convex subsets of the unit simplex. Moreover, vectors of Shapley values produce a convex set. In contrast to the imprecise probabilities, imprecise Shapley values are not a part of the unit simplex. Transferring definitions of reachable probability intervals to the above problem, we can write that conditions (15) imply that intervals $[\phi_i^L, \phi_i^U]$ are proper. This implies that the corresponding set of Shapley values is not empty. Moreover, it can be simply proved that bounds $\tilde{\phi}_k^L$ and $\tilde{\phi}_k^U$ are reachable. If the reachability condition is not satisfied, then intervals $[\phi_i^L, \phi_i^U]$ are unnecessarily broad. Moreover, they might be such that some values of the intervals do not correspond to condition (13). Proposition 1 gives a way to compute the

reachable intervals of Shapley values. At the same time, it can be extended to a more general case when we would like to find bounds for a linear function $g(\phi_1, \dots, \phi_m) = \sum_{i=1}^m a_i \phi_i = \langle \mathbf{a}, \phi \rangle$ of imprecise Shapley values. Here $\mathbf{a} = (a_1, \dots, a_m)$ is a vector of known coefficients, $\phi = (\phi_1, \dots, \phi_m)$. Intervals of $g(\phi|\mathbf{a})$ are computed by solving the following two linear programming problems (minimization and maximization):

$$g^L(\phi|\mathbf{a})(g^U(\phi|\mathbf{a})) = \min(\max) \langle \mathbf{a}, \phi \rangle,$$

subject to (13) and $\phi_k^L \leq \phi_k \leq \phi_k^U$, $k = 1, \dots, m$.

The dual optimization problems are

$$g^L(\phi|\mathbf{a}) = \max \left(D^L v_0 - D^U w_0 + \sum_{i=1}^m \phi_i^L v_i - \sum_{i=1}^m \phi_i^U w_i \right),$$

subject to

$$v_0 - w_0 + \sum_{i=1}^m (v_i - w_i) \leq a_k, \quad k = 1, \dots, m,$$

and

$$g^U(\phi|\mathbf{a}) = \min \left(D^U v_0 - D^L w_0 + \sum_{i=1}^m \phi_i^U v_i - \sum_{i=1}^m \phi_i^L w_i \right),$$

subject to

$$v_0 - w_0 + \sum_{i=1}^m (v_i - w_i) \geq a_k, \quad k = 1, \dots, m.$$

The above comments can be viewed as a starting point for development of a general theory of imprecise Shapley values. Moreover, Proposition 1 provides a tool for dealing with intervals of Shapley values without assumptions about sets \mathcal{P} of class probability distributions and about the distance D between the sets. Therefore, the next questions are to define imprecise statistical models producing sets \mathcal{P} and the corresponding distances D such that bounds (7)-(8) could be computed in a simple way. In order to answer these questions, we have to select a model producing \mathcal{P} and to select a distance D .

5.2 Imprecise statistical models

There are several imprecise models of probability distributions. One of the interesting models is the linear-vacuous mixture or the imprecise ε -contamination model [76]. It produces a set $\mathcal{P}(\varepsilon, P)$ of probabilities $P^* = (p_1^*, \dots, p_C^*)$ such that $p_i^* = (1 - \varepsilon)p_i + \varepsilon h_i$, where $P = (p_1, \dots, p_C)$ is an elicited probability distribution (in the considered case of SHAP, these distributions are $P_S, P_{S,i}, P_N$); $h_i \geq 0$ is arbitrary with $h_1 + \dots + h_C = 1$; $0 \leq \varepsilon \leq 1$. Parameter ε controls the size of set $\mathcal{P}(\varepsilon, P)$ and can be defined from size n of the training set. The greater the number of training examples, the less the uncertainty for probability distribution and the less the value of parameter ε . The set $\mathcal{P}(\varepsilon, P)$ is a subset of the unit simplex $S(1, C)$. Moreover, it

coincides with the unit simplex when $\varepsilon = 1$. According to the model, $\mathcal{P}(\varepsilon, P)$ is the convex set of probabilities with lower bound $(1 - \varepsilon)p_i$ and upper bound $(1 - \varepsilon)p_i + \varepsilon$, i.e.,

$$(1 - \varepsilon)p_i \leq p_i^* \leq (1 - \varepsilon)p_i + \varepsilon, \quad i = 1, \dots, C. \quad (18)$$

The convex set has C extreme points, which are all of the same form: the k -th element is given by $(1 - \varepsilon)p_i + \varepsilon$ and the other $T - 1$ elements are equal to $(1 - \varepsilon)p_i$, i.e.,

$$p_k^* = (1 - \varepsilon)p_k + \varepsilon, \quad p_i^* = (1 - \varepsilon)p_i, \quad i = 1, \dots, C, \quad i \neq k. \quad (19)$$

Fig. 4 illustrates sets $\mathcal{P}(\varepsilon, P_S)$, $\mathcal{P}(\varepsilon, P_{S,i})$, $\mathcal{P}(\varepsilon, P_N)$ for precise probability distributions P_S , $P_{S,i}$, P_N , respectively, in the form of large triangles around the corresponding distributions. Every distribution belonging to the sets can be a candidate for some “true” distribution which is actually unknown. The imprecise ε -contamination model is equivalent to the imprecise Dirichlet model (IDM) [77] to some extent. The IDM defined by [77] can be viewed as the set of all Dirichlet distributions over $\pi = (\pi_1, \dots, \pi_C)$ with parameters $\alpha = (\alpha_1, \dots, \alpha_C)$ and s such that the vector α belongs to the unit simplex and every α_i is the mean of π_i under the Dirichlet prior. Here π is the probability distribution defined on C events, for which the Dirichlet (s, α) prior is defined. For the IDM, the hyperparameter s determines how quickly upper and lower probabilities of events converge as statistical data accumulate. Smaller values of s produce faster convergence and stronger conclusions, whereas large values of s produce more cautious inferences. However, hyperparameter s should not depend on the number of observations. Let A be any non-trivial subset of a sample space, and let $n(A)$ denote the observed number of occurrences of A in the n trials. Then, according to [77], the predictive probability $P(A, s)$ under the Dirichlet posterior distribution is in the following interval

$$\underline{P}(A, s) = \frac{n(A)}{n + s}, \quad \bar{P}(A, s) = \frac{n(A) + s}{n + s}. \quad (20)$$

The hyperparameter s of the IDM and parameter ε of the imprecise ε -contamination model are connected as

$$\varepsilon = \frac{s}{n + s}. \quad (21)$$

Hence, one can see how ε depends on n by a fixed value of s . In particular, $\varepsilon = 1$, when $n = 0$, and $\varepsilon \rightarrow 0$, when $n \rightarrow \infty$.

5.3 Distances between subsets of probability distributions

In order to apply the SHAP method taking into account the imprecision of the class probability distributions, it is necessary to introduce the distance between probability distributions and to define a way for computing the largest and the smallest distances between all pairs of probability distributions which belong to the small subsets of distributions $\mathcal{P}(\varepsilon, P_S)$, $\mathcal{P}(\varepsilon, P_{S,i})$, $\mathcal{P}(\varepsilon, P_N)$.

There are a lot of distance measures between probability distributions. One of the most popular in machine learning measure is the Kullback-Leibler (KL) divergence or relative information [40]:

$$KL(P||Q) = \sum_{i=1}^C p_i \log \left(\frac{p_i}{q_i} \right).$$

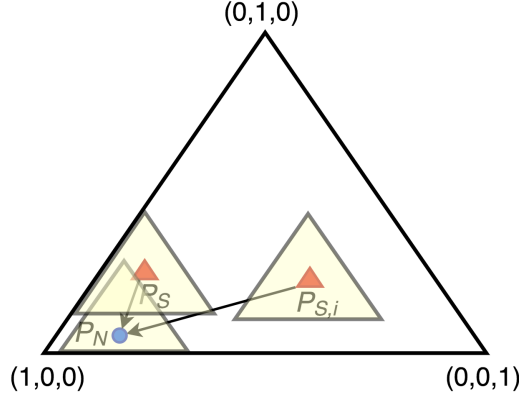


Figure 4: Illustration of distances between subsets produced by the imprecise ε -contamination model

This measure among other interesting measures, including relative J-divergence [23], relative Arithmetic-Geometric divergence [74], χ^2 -divergence [56], etc. [33, 74], can be derived using properties of Csiszar's f -divergence measure [19] which is of the form:

$$C_f(P||Q) = \sum_{i=1}^C q_i f\left(\frac{p_i}{q_i}\right),$$

where the function $f : (0, \infty) \rightarrow \mathbb{R}$ is convex and normalized, i.e., $f(1) = 0$, and it is assumed that $0 \cdot f(0/0) = 0$ and $0 \cdot f(p/0) = 0 = \lim_{q \rightarrow 0^+} qf(p/q)$. For example, functions $f(u) = -\ln u$ and $f(u) = (1 - u)^2/u$ generate the KL-divergence and the χ^2 -divergence [53], respectively.

5.4 A direct method to compute bounds for Shapley values

All the aforementioned distance measures lead to very complex optimization problems for computing bounds for distances between subsets of probability distributions. In order to avoid solving the optimization problems, Shapley values can be computed by means of generating a lot of points in subsets $\mathcal{P}(\varepsilon, P_S)$, $\mathcal{P}(\varepsilon, P_{S,i})$, $\mathcal{P}(\varepsilon, P_N)$ and computing the smallest and the largest distances or computing the smallest and the largest Shapley values.

There are many algorithms for generating uniformly distributed random points in the unit simplex [55, 65, 66]. One of the well-known and simple algorithms is of the form [66]:

1. Generate k independent unit-exponential random variables Y_1, \dots, Y_k and compute $T_k = \sum_{i=1}^k Y_i$.
2. Define $E_i = Y_i/T_k$ and return vector $E = (E_1, \dots, E_k)$ which is uniformly distributed in the unit simplex.

Note that set \mathcal{P} is convex, i.e., it is generated by finitely many linear constraints. This implies that it is totally defined by its extreme points or vertices denoted $\mathcal{E}(\mathcal{P})$. Suppose that

we have a set of r extreme points $Q_k = (q_1^{(k)}, \dots, q_C^{(k)})$ of the set \mathcal{P} , i.e., $q_k \in \mathcal{E}(\mathcal{P})$, $k = 1, \dots, r$. In the case of the imprecise ε -contamination model, there holds $r = C$. Then every probability distribution $P = (p_1, \dots, p_C)$ from \mathcal{P} can be represented as the linear combination of the extreme points

$$P = \sum_{k=1}^r \lambda_k \cdot Q_k. \quad (22)$$

Here $\lambda = (\lambda_1, \dots, \lambda_r)$ is a vector of weights such that $\lambda_1 + \dots + \lambda_r = 1$.

If to uniformly generate vectors λ from the unit simplex by using one of the known algorithms of generation, then random points P from the set \mathcal{P} can be obtained. Extreme points of set \mathcal{P} for the imprecise ε -contamination model are given in (19).

From all generated points in $\mathcal{P}(\varepsilon, P_S)$, $\mathcal{P}(\varepsilon, P_{S,i})$, $\mathcal{P}(\varepsilon, P_N)$, we select three corresponding points, say, $P_1 \in \mathcal{P}(\varepsilon, P_S)$, $R_1 \in \mathcal{P}(\varepsilon, P_{S,i})$, $Q_1 \in \mathcal{P}(\varepsilon, P_N)$ such that the difference $D(P, Q) - D(R, Q)$ of distances achieves its minimum. These points contribute into the lower Shapley value ϕ_i^L . In the same way, three points P_2, R_2, Q_2 are selected from the same sets, respectively, such that the difference $D(P, Q) - D(R, Q)$ achieves its maximum. These points contribute into the upper Shapley value ϕ_i^U . This procedure is repeated for all Shapley values ϕ_i , $i = 1, \dots, m$.

The main advantage of the above generation approach for computing the lower and upper Shapley values is that an arbitrary distance between probability distributions can be used for implementing the approach, for example, the KL divergence or the χ^2 -divergence. There are no restrictions for selecting distances. Moreover, intervals for Shapley values can be also directly computed. Of course, this approach may be extremely complex especially when training examples have a high dimension and parameter ε of the imprecise ε -contamination model is rather large (the imprecise model produces large sets $\mathcal{P}(\varepsilon, \cdot)$). Moreover, it is difficult to control the accuracy of the obtained Shapley values because there is a chance that the selected points P_1, R_1, Q_1 and P_2, R_2, Q_2 may be not optimal, i.e., the corresponding differences $D(P, Q) - D(R, Q)$ do not achieve the minimum and the maximum. In order to overcome this difficulty, another approach is proposed, which is based on applying the Kolmogorov-Smirnov distance leading to a set of very simple linear programming problems.

6 The Kolmogorov-Smirnov distance and the imprecise SHAP

The Kolmogorov-Smirnov distance between two probability distributions $P = (p_1, \dots, p_C)$ and $Q = (q_1, \dots, q_C)$ is defined as the maximal distance between the cumulative distributions. Let $\pi = (\pi_1, \dots, \pi_C)$ and $\alpha = (\alpha_1, \dots, \alpha_C)$ be cumulative probability distributions corresponding to the distributions P and Q , respectively, where $\pi_i = \sum_{j=1}^i p_j$ and $\alpha_i = \sum_{j=1}^i q_j$. It is assumed that $\pi_C = \alpha_C = 1$. Then the Kolmogorov-Smirnov distance is of the form:

$$D_{KS}(P, Q) = \max_{i=1, \dots, C-1} |\pi_i - \alpha_i|. \quad (23)$$

An imprecise extension of the Kolmogorov-Smirnov distance with using the imprecise ε -contamination model has been studied by Montes et al. [50]. However, we consider the corre-

sponding distances as elements of optimization problems for computing lower and upper bounds for Shapley values.

First, we extend the definition of the imprecise ε -contamination model $p_i^* = (1 - \varepsilon)p_i + \varepsilon h_i$ on the case of probabilities of arbitrary events A . The model defines $P^*(A)$ in the same way, i.e.,

$$P^*(A) = (1 - \varepsilon)P(A) + \varepsilon H(A), \quad (24)$$

where $P(A)$ is an elicited probability of event A , $H(A)$ is the probability of A under condition of arbitrary distribution.

This implies that bounds for $P^*(A)$ are defined as follows:

$$(1 - \varepsilon)P(A) \leq P^*(A) \leq (1 - \varepsilon)P(A) + \varepsilon. \quad (25)$$

If $A = \{1, 2, \dots, i\}$, then $P^*(A)$ is the i -th cumulative probability. Hence, we can define bounds for cumulative probability distributions. Denote sets of cumulative probability distributions π, τ, α produced by the imprecise ε -contamination model for the distributions $P_S, P_{S,i}, P_N$ as $\mathcal{R}(\varepsilon, P_S), \mathcal{R}(\varepsilon, P_{S,i}), \mathcal{R}(\varepsilon, P_N)$, respectively. It is supposed that the lower and upper bounds for probabilities $\pi_i, \tau_i, \alpha_i, i = 1, \dots, C - 1$, are

$$\pi_i^L \leq \pi_i \leq \pi_i^U, \quad \tau_i^L \leq \tau_i \leq \tau_i^U, \quad \alpha_i^L \leq \alpha_i \leq \alpha_i^U. \quad (26)$$

We assume that $\pi_C = \tau_C = \alpha_C = 1$ because these values represent the cumulative distribution function.

Let us consider the lower bound L for $D_{KS}(P, Q) - D_{KS}(R, Q)$. It can be derived from the following optimization problem:

$$L = \min_{\pi, \tau, \alpha} \left(\max_{i=1, \dots, C-1} |\pi_i - \alpha_i| - \max_{i=1, \dots, C-1} |\tau_i - \alpha_i| \right), \quad (27)$$

subject to (26).

This is non-convex optimization problem. However, it can be represented as a set of $2(C - 1)$ simple linear programming problems.

Proposition 2 *The lower bound L for $D_{KS}(P, Q) - D_{KS}(R, Q)$ or the solution of problem (27) is determined by solving $2(C - 1)$ linear programming problems:*

$$L_1(k) = \min_{B, \pi, \alpha} (B - \tau_k^U + \alpha_k), \quad k = 1, \dots, C - 1, \quad (28)$$

$$L_2(k) = \min_{B, \pi, \alpha} (B - \alpha_k + \tau_k^L), \quad k = 1, \dots, C - 1, \quad (29)$$

subject to

$$\pi_i^L \leq \pi_i \leq \pi_i^U, \quad \alpha_i^L \leq \alpha_i \leq \alpha_i^U, \quad i = 1, \dots, C - 1, \quad (30)$$

$$B \geq \pi_i - \alpha_i, \quad B \geq \alpha_i - \pi_i, \quad i = 1, \dots, C - 1, \quad (31)$$

$$\pi_i \leq \pi_{i+1}, \quad \alpha_i \leq \alpha_{i+1}, \quad i = 1, \dots, C - 2, \quad (32)$$

For $L_1(k)$, the following constraints are added:

$$\alpha_k \leq \tau_k^U \text{ and } \tau_k^U - \alpha_k \geq \tau_i^U - \alpha_i, i = 1, \dots, C-1, i \neq k. \quad (33)$$

For $L_2(k)$, then the following constraints are added:

$$\alpha_k \geq \tau_k^L \text{ and } \alpha_k - \tau_k^L \geq \alpha_i - \tau_i^L, i = 1, \dots, C-1, i \neq k. \quad (34)$$

A final solution is determined by selecting $k_1 = \arg \max_k (\tau_k^U - \alpha_k)$ from (28) and $k_2 = \arg \max_k (\alpha_k - \tau_k^L)$ from (29). The lower bound is

$$L = \begin{cases} L_1(k_1), & \text{if } \tau_{k_1}^U - \alpha_{k_1} \geq \alpha_{k_2} - \tau_{k_2}^L, \\ L_2(k_2), & \text{otherwise.} \end{cases} \quad (35)$$

It should be noted that problems (28) do not have solutions for some k when inequality $\tau_k^U < \alpha_k^L$ is valid. This follows from constraints $\alpha_k \leq \tau_k^U$ in (33) and $\alpha_k^L \leq \alpha_k$ in (30). The same can be said about solutions of problems (29). They do not have solutions when inequality $\tau_k^L > \alpha_k^U$ is valid. This follows from constraints $\alpha_k \geq \tau_k^L$ in (34) and $\alpha_k \leq \alpha_k^U$ in (30).

Let us consider now the upper bound U for $D_{KS}(P, Q) - D_{KS}(R, Q)$. It can be derived from the following optimization problem:

$$U = \max_{\pi, \tau, \alpha} \left(\max_{i=1, \dots, C-1} |\pi_i - \alpha_i| - \max_{i=1, \dots, C-1} |\tau_i - \alpha_i| \right), \quad (36)$$

subject to (26).

Proposition 3 *The upper bound U for $D_{KS}(P, Q) - D_{KS}(R, Q)$ or the solution of problem (36) is determined by solving $2C - 1$ linear programming problems:*

$$U_1(k) = \max_{B, \tau, \alpha} (\pi_k^U - \alpha_k - B), \quad k = 1, \dots, C-1, \quad (37)$$

$$U_2(k) = \max_{B, \tau, \alpha} (\alpha_k - \pi_k^L - B), \quad k = 1, \dots, C-1, \quad (38)$$

subject to

$$\tau_i^L \leq \tau_i \leq \tau_i^U, \alpha_i^L \leq \alpha_i \leq \alpha_i^U, \quad i = 1, \dots, C-1, \quad (39)$$

$$B \geq \tau_i - \alpha_i, \quad B \geq \alpha_i - \tau_i, \quad i = 1, \dots, C-1, \quad (40)$$

$$\tau_i \leq \tau_{i+1}, \quad \alpha_i \leq \alpha_{i+1}, \quad i = 1, \dots, C-2, \quad (41)$$

For $L_1(k)$, the following constraints are added:

$$\alpha_k \leq \pi_k^U \text{ and } \pi_k^U - \alpha_k \geq \pi_i^U - \alpha_i, \quad i = 1, \dots, C-1, \quad i \neq k. \quad (42)$$

For $L_2(k)$, the following constraints are added:

$$\alpha_k \geq \pi_k^L \text{ and } \alpha_k - \pi_k^L \geq \alpha_i - \pi_i^L, \quad i = 1, \dots, C-1, \quad i \neq k. \quad (43)$$

A final solution is determined by selecting $k_1 = \arg \max_k (\pi_k^U - \alpha_k)$ from (37) and $k_2 = \arg \max_k (\alpha_k - \pi_k^L)$ from (38). The upper bound is

$$U = \begin{cases} U_1(k_1), & \text{if } \pi_{k_1}^U - \alpha_{k_1} \geq \alpha_{k_2} - \pi_{k_2}^L, \\ U_2(k_2), & \text{otherwise.} \end{cases} \quad (44)$$

It should be noted that problems (37) do not have solutions for some k when inequality $\pi_k^U < \alpha_k^L$ is valid. This follows from constraints $\alpha_k^L \leq \alpha_k$ in (39) and $\alpha_k \leq \pi_k^U$ in (42). The same can be said about solutions of problems (38). They do not have solutions when inequality $\pi_k^L \geq \alpha_k^U$ is valid. This follows from constraints $\alpha_k \leq \alpha_k^U$ in (39) and $\alpha_k \geq \pi_k^L$ in (43).

The Kolmogorov-Smirnov distance for the binary classification black-box model is of the form:

$$D_{KS}(P, Q) = |\pi_1 - \alpha_1|. \quad (45)$$

$$L = \min_{\pi, \tau, \alpha} (|\pi_1 - \alpha_1| - |\tau_1 - \alpha_1|), \quad (46)$$

The index 1 will be omitted below for short.

Corollary 4 *For the binary classification black-box model with $C = 2$, the lower L and upper U bounds for $D_{KS}(P, Q) - D_{KS}(R, Q)$ are*

$$L = \begin{cases} 2\alpha^L - \pi^U - \tau^U, & \text{if } \pi^U \leq \alpha^L \leq \tau^U, \\ \pi^L - \tau^U, & \text{if } \alpha^L \leq \min(\tau^U, \pi^L), \\ \tau^L - \pi^U, & \text{if } \alpha^U \geq \max(\tau^L, \pi^U), \\ \pi^L + \tau^L - 2\alpha^U, & \text{if } \tau^L \leq \alpha^U \leq \pi^L, \end{cases} \quad (47)$$

$$U = \begin{cases} 2\alpha^U - \pi^L - \tau^L, & \text{if } \pi^L \leq \alpha^U \leq \tau^L, \\ \pi^U - \tau^L, & \text{if } \alpha^U \leq \min(\tau^L, \pi^U), \\ \tau^U - \pi^L, & \text{if } \alpha^L \geq \max(\tau^U, \pi^L), \\ \pi^U + \tau^U - 2\alpha^L, & \text{if } \tau^U \leq \alpha^L \leq \pi^U. \end{cases} \quad (48)$$

It follows from (47) and (48) that there holds for the case of precise probabilities:

$$D_{KS}(P, Q) - D_{KS}(R, Q) = |\pi - \alpha| - |\tau - \alpha|. \quad (49)$$

The next question is how to compute bounds D^L and D^U for D in (13), which are used to reduce intervals of Shapley values.

Let π and α be cumulative distribution functions corresponding to P_\emptyset and P_N defined in (6), respectively, i.e., $\pi \in P_\emptyset$ and $\alpha \in P_N$. Then the lower bound D^L is determined

$$D^L = \min_{\pi, \alpha} \max_{i=1, \dots, C-1} |\pi_i - \alpha_i|. \quad (50)$$

The upper bound D^U is determined from the following optimization problem:

$$D^U = \max_{\pi, \alpha} \max_{i=1, \dots, C-1} |\pi_i - \alpha_i|. \quad (51)$$

Proposition 5 *The lower bound D^L is determined from the following linear programming problem:*

$$D^L = \min_{\pi, \alpha} B, \quad (52)$$

subject to (30)-(32).

The upper bound D^U is determined as

$$D^U = \max_{k=1, \dots, C-1} \max(\pi_k^U - \alpha_k^L, \alpha_k^U - \pi_k^L). \quad (53)$$

Dataset	Classes	Training	Testing
1	2	879, 121	215, 35
2	3	340, 336, 324	92, 80, 78
3	4	249, 263, 238, 250	64, 50, 74, 62

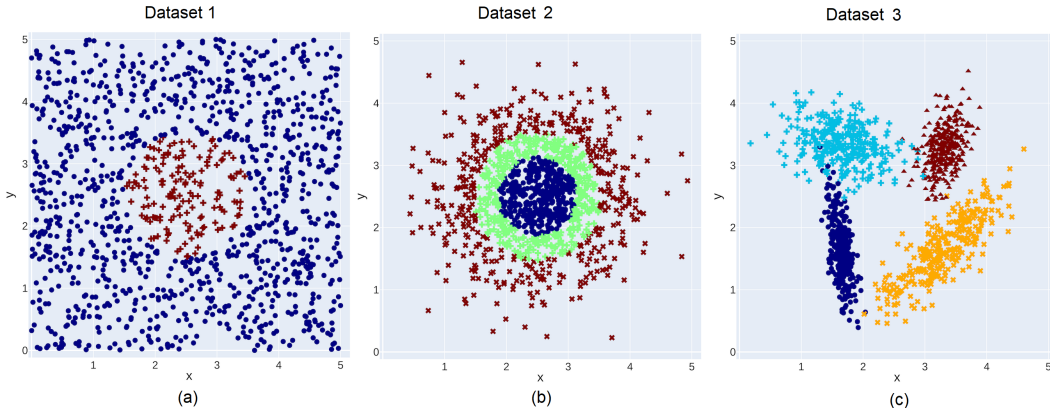


Figure 5: Three synthetic datasets for numerical experiments

Finally, we have obtained basic tools for dealing with imprecise Shapley values, which include Propositions 2, 3, and 5.

7 Numerical experiments

In all numerical experiments, the black-box model is the random forest consisting of 100 decision trees with largest depth 8. The choice of the random forest is due to simplicity of getting the class probabilities.

7.1 Numerical experiments with synthetic data

In order to study properties of the imprecise SHAP and to compare its predictions with the original SHAP, we generate three datasets of synthetic data. Every dataset consists of 1000 training examples and 250 testing examples such that every example is characterized by two features (x and y). The datasets are described in Table 1 where the second column shows the number of classes, numbers of training and testing examples in the classes are given in the third and fourth columns, respectively.

Every example of the first dataset is randomly generated from the uniform distribution in $[0, 5] \times [0, 5]$. Points inside a circle with the unit radius and center $(2.5, 2.5)$ belongs to the first class, other points belongs to the second class. Points of the dataset are shown in Fig. 5 (a).

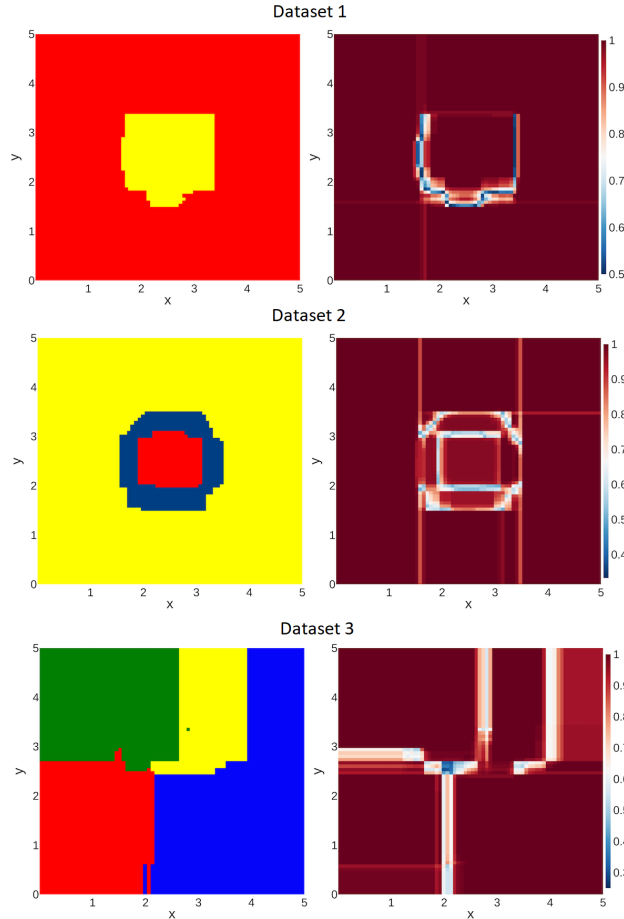


Figure 6: Predictions of the black-box random forest for three datasets (three rows of pictures), the left picture in every row depicts predicted classes, the right picture depicts heatmaps of largest probabilities of predicted classes

Every example of the second dataset is randomly generated from the normal distribution with the expectation $(2.5, 2.5)$ and the covariance matrix $0.5 \cdot \mathbf{I}$, where \mathbf{I} is the unit matrix. Points inside a circle with the unit radius and center $(2.5, 2.5)$ belongs to the first class. Points located outside the circle with radius 2 and center $(2.5, 2.5)$ belong to the third class. Other points belong to the second class. Points of the dataset are shown in Fig. 5 (b).

Every example of the third dataset is randomly generated in accordance with a procedure implemented in the Python library “sklearn” in function “sklearn.datasets.make_classification”. According to the procedure, clusters of points normally distributed with the variance 1 about vertices of the square with sides of length 2 are generated. Details of the generating procedure can be found in https://scikit-learn.org/stable/modules/generated/sklearn.datasets.make_classification.html. Points of the dataset are shown in Fig. 5 (c).

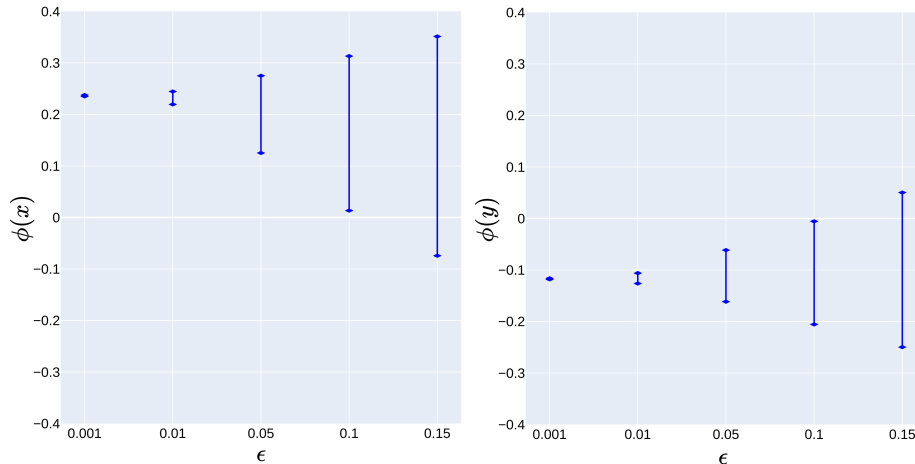


Figure 7: Intervals of Shapley values for point (1.5, 2.5) from the first synthetic dataset with two features, x and y , for different contamination parameters ϵ

Predictions of the black-box random forest for every dataset are illustrated in Fig. 6 where every row of pictures corresponds to a certain dataset, the first column of pictures depicts predicted classes by different colors for every dataset, the second column depicts heatmaps corresponding to largest probabilities of predicted classes. It is clearly seen from the second column of pictures in Fig. 6 that the black-box random forest cannot cope with examples which are close to boundaries between classes.

An example of interval-valued Shapley values as functions of the contamination parameter ϵ is shown in Fig. 7. The testing example with features (1.5, 2.5) is chosen because this point is very close to the boundary between classes and the corresponding class distribution is non-trivial. Moreover, the location of the point simply shows that feature x is important because its small perturbation changes the class (see Fig. 5 (a)) in contrast to feature y which does not change the class. One can see from Fig. 7 that intervals of Shapley values for feature x are clearly larger than the intervals for y . At the same time, intervals for Shapley values of x and y are intersecting when $\epsilon = 0.15$. However, the intersecting area is rather small, therefore, we can confidently assert that feature x is more important. Another analyzed point is (2.5, 2.5). It is seen from Fig. 5 (a) that this point is in the center of the circle, and both the features equally contribute into the prediction. The same can be concluded from Fig. 8 where intervals of Shapley values are shown. One can see from Fig. 8 that the obtained intervals are more narrow than the same intervals given in Fig. 7.

Moreover, the above experiments clearly show that the approach for computing contributions of every feature based on the difference of distances $D(P_S, P_N) - D(P_{S,i}, P_N)$ provides correct results which are consistent with the visual relationship between features and predictions depicted in Fig. 6.

Similar examples can be given for the second and the third synthetic datasets. In particular, Fig. 9 shows intervals of Shapley values corresponding two features, x and y , when the black-

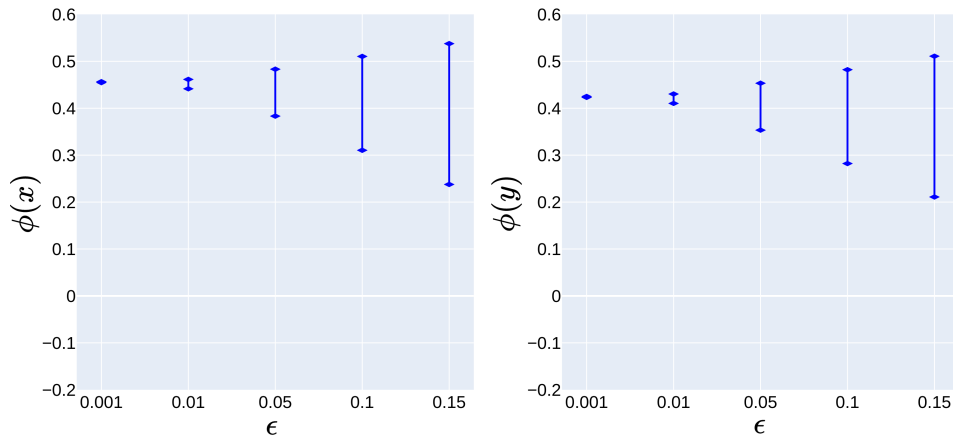


Figure 8: Intervals of Shapley values for point (2.5, 2.5) from the first synthetic dataset with two features, x and y , for different contamination parameters ϵ

box random forest predicts point (3.5, 1.5) located close to the class boundary (see Fig. 5 (b)). One can see again that the interval relationship corresponds to the visual relationship between features and predictions depicted in Fig. 6. Fig. 10 shows intervals of Shapley values for point (4.5, 4.5) located far from the class boundary (see Fig. 5 (b)).

Figs. 11-12 show similar pictures for the third synthetic dataset where predictions corresponding to points (4.0, 4.0) and (1.0, 1.0) are explained. It is interesting to point out that the case of point (4.0, 4.0). If we look at Fig. 5 (c), then we see that point belong to the area of one of the classes. This implies that the corresponding prediction almost equally depends on x and y . However, if we look at Fig. 6 (the third row), then we see that the classifier does not provide a certain class as a prediction, and the explainer selects feature x as the most important one assuming that y does not change the class though this is not obvious from Fig. 5 (c). This observation is justified by the fact that intervals of Shapley values for x are the largest ones for all $\epsilon > 0$, i.e., imprecision of the corresponding prediction impacts on imprecision of Shapley values.

Fig. 13 illustrates cases of the Shapley value interval relationship for $\epsilon = 0.15$ (blue segments) and for $\epsilon = 0$ (red circles) for the third dataset. If to consider the precise Shapley values, then the first case (the left picture) shows that feature x is more important than feature y because the corresponding red circle for x is higher than the circle for y . At the same time, a part of the interval of x for $\epsilon = 0.15$ is smaller than the interval of y . This implies that the decision made by using only the precise values of Shapley values may be incorrect. A similar case is depicted in the right picture of Fig. 13. Many such cases can be provided, which illustrate that imprecise Shapley values should be studied instead of precise values because intervals show all possible Shapley values for every feature and can reduce mistakes related to the incorrect explanation.

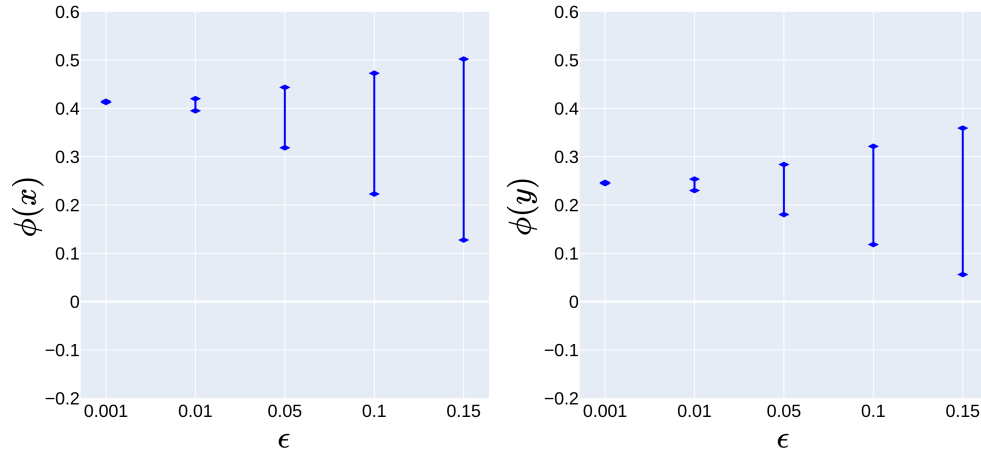


Figure 9: Intervals of Shapley values for point $(3.5, 1.5)$ from the second synthetic dataset with two features, x and y , for different contamination parameters ϵ

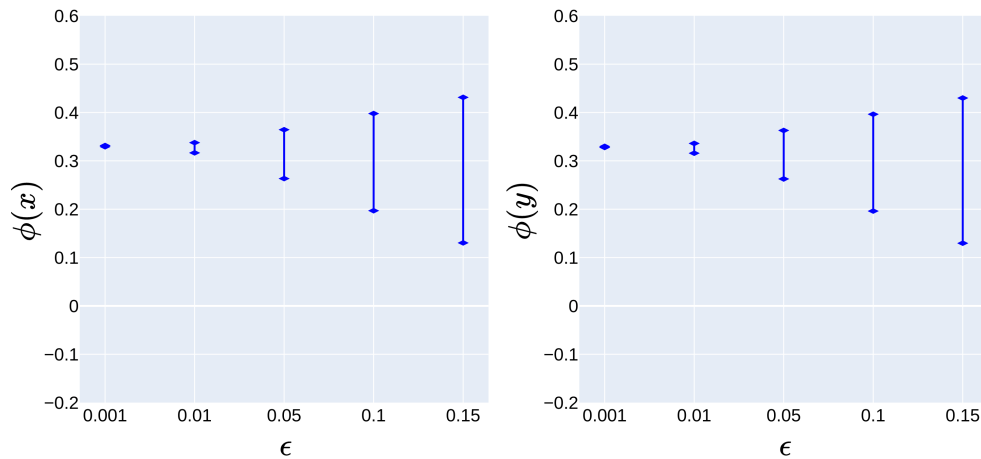


Figure 10: Intervals of Shapley values for point $(4.5, 4.5)$ from the second synthetic dataset with two features, x and y , for different contamination parameters ϵ

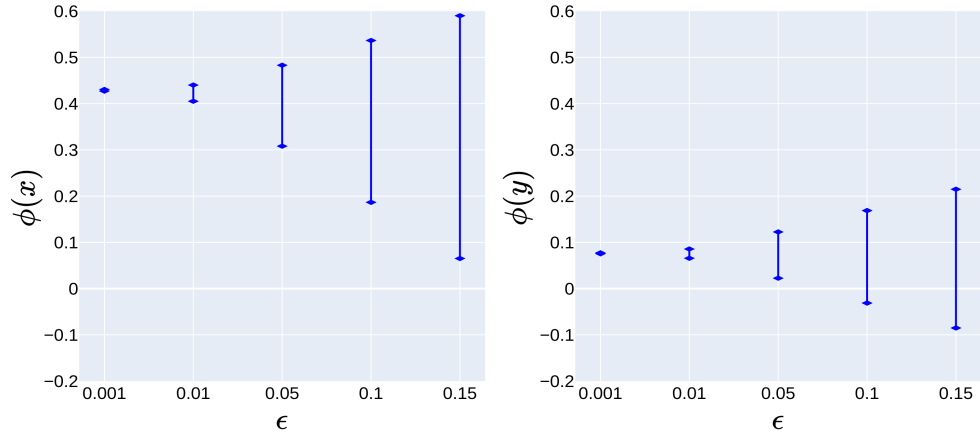


Figure 11: Intervals of Shapley values for point (4.0, 4.0) from the third synthetic dataset with two features, x and y , for different contamination parameters ϵ

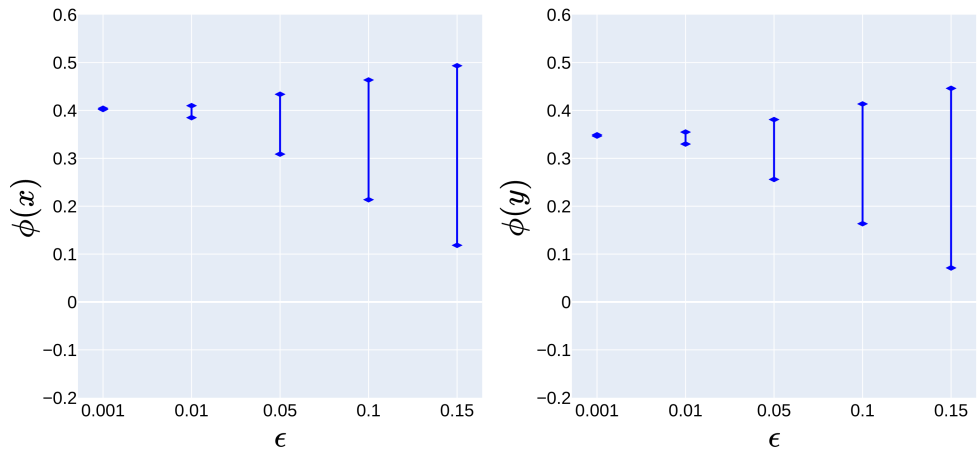


Figure 12: Intervals of Shapley values for point (1.0, 1.0) from the third synthetic dataset with two features, x and y , for different contamination parameters ϵ

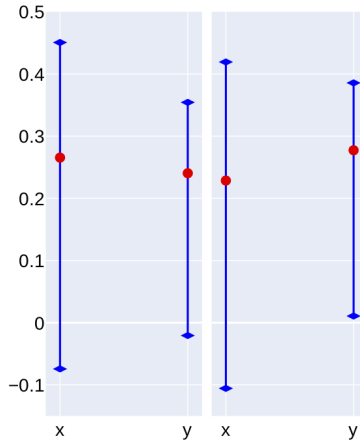


Figure 13: Intervals of Shapley values for two points (2.8, 1.5) and (1.84, 3.34)

7.2 Numerical experiments with real data

In order to illustrate the Imprecise SHAP, we investigate the model for data sets from UCI Machine Learning Repository [42]. We consider datasets: Seeds (<https://archive.ics.uci.edu/ml/datasets/seeds>), $m = 7$, $n = 210$, $C = 3$; Glass Identification (<https://archive.ics.uci.edu/ml/datasets/glass+identification>), $m = 10$, $n = 214$, $C = 7$; Ecoli (<https://archive.ics.uci.edu/ml/datasets/ecoli>), $m = 8$, $n = 336$, $C = 8$. More detailed information can be found from, respectively, the data resources.

As an example, Fig. 14 illustrates intervals of Shapley values for random point (16.7, 14.7, 0.9, 6.4, 3.5, 2.5, 5.6) from the Seeds dataset by contamination parameter $\epsilon = 0.15$. Features are denoted as follows: area (area), perimeter (per), compactness (comp), length of kernel (len_ker), width of kernel (width), asymmetry coefficient (asym), length of kernel groove (len_gr). Red circles, which are close to centers of intervals, show precise Shapley values obtained for $\epsilon = 0$. It can be seen from Fig. 14 that feature “len_gr” provides the highest contribution to the corresponding prediction. In this case, the relationship between intervals mainly coincides with the relationship between precise values. However, every point in the intervals may be regarded as a true contribution value, therefore, there is a chance that feature “len_gr” does not maximally contribute to the prediction. Another example for random point (18.1, 16.1, 0.88, 6.06, 3.56, 3.62, 6.0) by the same ϵ is shown in Fig. 15 where the relationship between imprecise Shapley values is more explicit.

Table 2 shows the original SHAP results (<https://github.com/slundberg/shap>) and is provided for comparison purposes. Its cell (i, j) contains the value of the Shapley value for the j -th feature under condition that the prediction is the i -th class probability. Table 2 also shows that feature “len_gr” has the largest contribution to the first and to the second classes. This result correlates with the results shown in Fig. 15.

Fig. 16 shows intervals of Shapley values for random point (0.8, 0.8, 0.65, 0.6, 0.17, 0.45, 0.85) from the Ecoli dataset by contamination parameter $\epsilon = 0.15$. Features are denoted in accor-

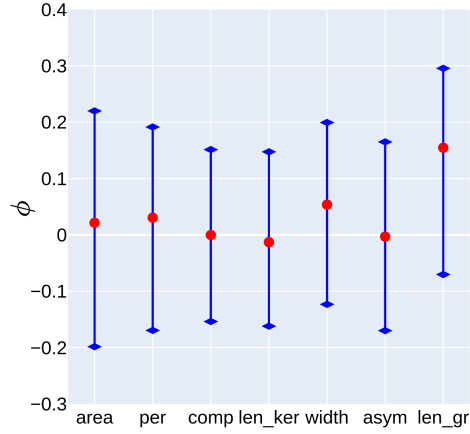


Figure 14: Intervals of Shapley values for $\varepsilon = 0.15$ for the first random point from the Seeds dataset

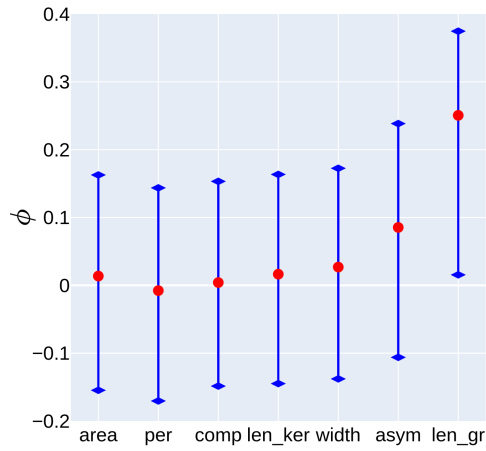


Figure 15: Intervals of Shapley values for $\varepsilon = 0.15$ for the second random point from the Seeds dataset

Table 2: The original SHAP results for the Seeds dataset and the second random point

Features	Class 1	Class 2	Class 3
area	-0.019	0.108	-0.088
per	-0.036	0.109	-0.073
comp	0.005	0.001	-0.006
len_ker	-0.080	0.128	-0.048
width	0.011	0.04	-0.051
asym	-0.023	0.018	0.006
len_gr	-0.205	0.254	-0.049

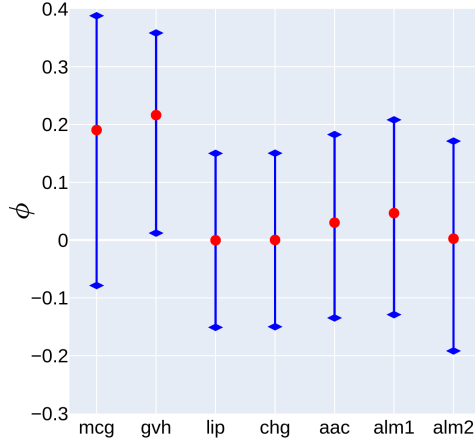


Figure 16: Intervals of Shapley values for $\varepsilon = 0.15$ for the first random point from the Ecoli dataset

dance with the data resources as follows: mcg, gvh, lip, chg, aac, alm1, alm2. It can be seen from Fig. 16 that two features “mcg” and “gvh” provide the highest contribution to the corresponding prediction. However, it is difficult to select a single feature among features “mcg” and “gvh”. From the one hand, “gvh” is more important if we assume that $\varepsilon = 0$. On the other hand, the corresponding interval of the Shapley value included in interval of “mcg”. This example clearly illustrates that the use of imprecise Shapley values may change our decision about the feature contributions. Another example for random point $(0.5, 0.79, 0.8, 0.6, 0.8, 0.58, 0.3)$ by the same ε is shown in Fig. 17 where we have the same problem of the feature selection among features “gvh” and “lip”. Moreover, one can see from Fig. 17 that features “aac” and “alm1” can be also viewed as important ones. This implies that imprecise Shapley values show a more correct relationship of the feature contributions.

Fig. 18 shows intervals of Shapley values for random point $(1.53, 16, 2.15, 0.56, 72, 3.6, 13.1, 0.07, 0.005)$ from the Glass Identification dataset by contamination parameter $\varepsilon = 0.15$. Features are denoted in accordance with the data resources as follows: RI, Na, Mg, Al, Si, K, Ca, Ba, Fe. This numerical example is also demonstrative. One can see from Fig. 18 that feature “Ca” is the most important under condition $\varepsilon = 0$. However, the interval of this feature is comparable with other intervals especially with the interval of feature “Mg”. In contrast to this numerical example, imprecise Shapley values obtained for another random point $(1.51, 13, 0.6, 1.6, 75, 4.5, 6.6, 0.06, 0.02)$ shown in Fig. 19 strongly imply that feature “Mg” is the most important one.

The above experiments have illustrated importance of the imprecise SHAP as a method for taking into account possible aleatoric uncertainty of predictions due to the limited amount of training data or other reasons. We could see from the experiments that the precise explanation may differ from the imprecise explanation. It should be noted that decision making based on intervals is ambiguous. It depends on a selected decision strategy. In particular, the well-known way for dealing with imprecise data is to use pessimistic or robust strategy. In accordance with

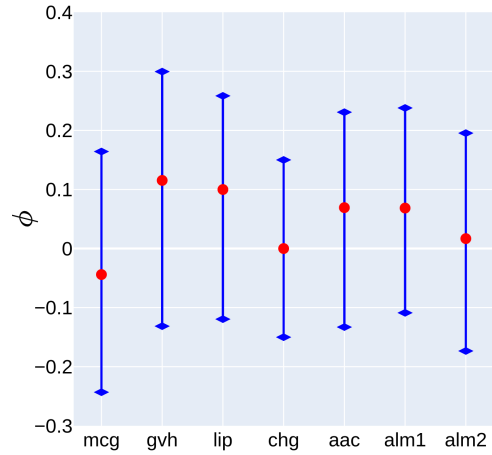


Figure 17: Intervals of Shapley values for $\varepsilon = 0.15$ for the second random point from the Ecoli dataset

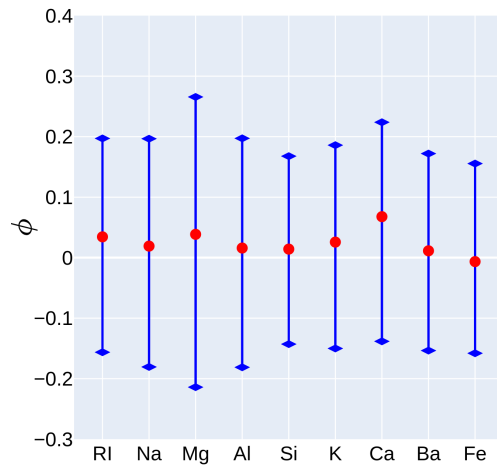


Figure 18: Intervals of Shapley values for $\varepsilon = 0.15$ for the first random point from the Glass Identification dataset

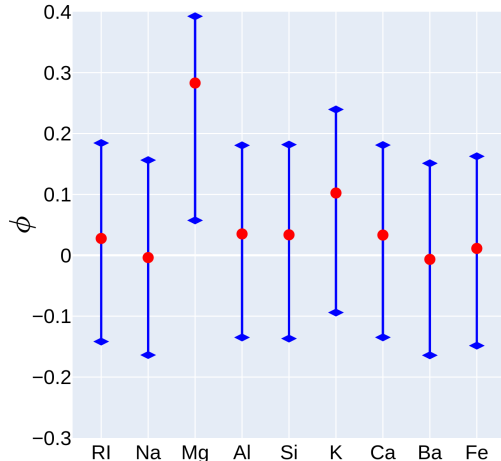


Figure 19: Intervals of Shapley values for $\varepsilon = 0.15$ for the second random point from the Glass Identification dataset

this strategy, if we are looking for the largest values of contributions, then lower bounds of intervals are considered and compared. If we are looking for unimportant features to remove them, then upper bounds of intervals should be considered. For example, it follows from the resulting imprecise Shapley values obtained for the second random point from the Ecoli dataset, which are shown in Fig. 17, the robust strategy selects feature “alm1” as the most important one though the most important intervals by using precise Shapley values ($\varepsilon = 0$) provide three different important features: “gvh”, “lip” and “aac”. The robust strategy can be interpreted as an insurance against the worst case [62]. Another “extreme” strategy is optimistic. It selects the upper bounds of intervals. The optimistic strategy cannot be called robust. There are other strategies, for example, the cautious strategy for which the most important feature is defined as

$$\arg \max_{i=1,\dots,m} (\eta \phi_i^L + (1 - \eta) \phi_i^U). \quad (54)$$

Here η is a cautious parameter taking values from 0 to 1. The case $\eta = 1$ corresponds to the robust decision strategy.

The choice of a certain strategy depends on a considered application and can be regarded as a direction for further research.

8 Conclusion

A new approach to explanation of the black-box machine learning model probabilistic predictions has been proposed, which aims to take into account the imprecision of probabilities composing the predictions. It can be applied to explanation of various machine learning models. In addition to multiclassification models, we have to point out a class of survival models, for example, the survival SVM [11], random survival forests [32, 78], survival neural networks [24, 36],

where this approach can be successfully used. Their predictions are survival functions which are usually represented as stepwise functions due to a finite number of the event observation times. Differences between steps of every survival function produce a probability distribution. Due to a limited amount of data, we get imprecise survival functions which have to be explained. A modification of LIME called SurvLIME-KS [38] has been developed to solve the survival model explanation problem under incomplete data. However, SurvLIME-KS provides precise minimax coefficients of the LIME linear regression which try to explain the worst case of the survival function from a set of functions. Sometimes, it is useful to have interval-valued estimates, which characterize the coefficients themselves as well as their uncertainty (the interval width), instead of the robust values because it is difficult to interpret the robustness itself. The proposed approach allows us to get interval-valued Shapley values which have these properties.

It is important to point out that the presented results are general and do not directly depend on the imprecise statistical model which describes imprecision of predictions. At the same time, a specific implementation of the approach requires choosing an imprecise model. In particular, bounds for π_i , τ_i , α_i , $i = 1, \dots, C - 1$, are defined by (25) which is given for the imprecise ε -contamination model. The investigation how different imprecise models impact on the explanation results can be regarded as a direction for further research. The same concerns with the Kolmogorov-Smirnov distance. The approach adaptation to different probability distribution distances is another direction for research.

A direction for further research is to study how to combine the obtained intervals explaining predictions on parts of intervals to reduce the SHAP complexity. This idea is mainly based on using an ensemble of random SHAPs [75] where the ensemble consists of many SHAPs such that every SHAP explains only a part of features.

Acknowledgement

This work is supported by the Russian Science Foundation under grant 21-11-00116.

Appendix

Proof of Proposition 1: Suppose that the sum $\sum_{i=1}^m \phi_i$ is precise and equals to $t \in [D^L, D^U]$. First, we consider the upper bound $\tilde{\phi}_k^U$ for ϕ_k . Then the optimization problem is of the form:

$$\tilde{\phi}_k^U = \max \phi_k, \tag{55}$$

subject to

$$\sum_{i=1}^m \phi_i = t, \tag{56}$$

$$\phi_i^L \leq \phi_i \leq \phi_i^U, \phi_i \geq 0, i = 1, \dots, m. \tag{57}$$

Let us write the dual problem. It is of the form:

$$\tilde{\phi}_k^U = \min \left(t \cdot w_0 + \sum_{i=1}^m \phi_i^U \cdot v_i - \sum_{i=1}^m \phi_i^L \cdot w_i \right), \quad (58)$$

subject to

$$w_0 + (v_i - w_i) \geq \mathbf{1}_k(i), \quad i = 1, \dots, m, \quad (59)$$

$$v_i \geq 0, \quad w_i \geq 0, \quad i = 1, \dots, m. \quad (60)$$

Here $w_0 \in \mathbb{R}$, $v_i \in \mathbb{R}_+$, $w_i \in \mathbb{R}_+$ are optimization variables; $\mathbf{1}_k(i)$ is the indicator function taking value 1 if $k = i$. The problem has $2m + 1$ variables and $3m$ constraints. It is well-known from the linear programming theory that $2m + 1$ constraints among all constraints are equalities. It is simply to prove that either $v_i = 0$ or $w_i = 0$. Suppose that the k -th constraint is one of the equalities. Suppose also that $v_k = 1$ and $w_k = 0$ (only for the k -th constraint). To minimize the objective function, w_0 should be as small as possible. The assumption $\phi_i^L \geq 0$ for all i is used here. It follows from the k -th constraint that $w_0 = 0$. Then all variables v_i , w_i are zero. Substituting the values into objective function, we get the first solution $\tilde{\phi}_k^U = \phi_k^U$. Another solution when the k -th constraint is one of the equalities is obtained if $w_0 = 1$, $v_k = 0$, $w_k = 1$. In this case, $v_i = 0$ and $w_i = 1$ for all $i \neq k$. Hence, there holds

$$\tilde{\phi}_k^U = t - \sum_{i=1}^m \phi_i^L. \quad (61)$$

Other combinations of equalities lead to a larger objective function. In sum, we get the solution of problem (58)-(60):

$$\tilde{\phi}_k^U = \min \left(\phi_k^U, t - \sum_{i=1}^m \phi_i^L \right). \quad (62)$$

The solution is valid for all t from interval $[D^L, D^U]$. This implies that the smallest $\tilde{\phi}_k^U$ is achieved when $t = D^L$, and we get (16). The same approach can be used to derive the lower bound $\tilde{\phi}_i^L$ which is given in (17) as was to be proved.

Proof of Proposition 2: Introduce a new variable $B = \sup_{i=1, \dots, C-1} |\pi_i - \alpha_i|$. Then problem (27) becomes

$$\min_{\pi, \tau, \alpha} \left(B - \sup_{i=1, \dots, C-1} |\tau_i - \alpha_i| \right), \quad (63)$$

subject to (26) and (32).

Constraints (32) mean that π_i and α_i are elements of the cumulative distribution functions. Suppose that the largest value of $|\tau_i - \alpha_i|$ is achieved for some index k , i.e.,

$$k = \arg \max_i |\tau_i - \alpha_i|. \quad (64)$$

Then we can rewrite the objective function for the given k as

$$\min_{\pi, \tau, \alpha} (B - |\tau_k - \alpha_k|). \quad (65)$$

To achieve the minimum of the objective function, the term $|\tau_k - \alpha_k|$ has to be maximized. Since, the cumulative distribution τ does not depend on π and α , then the maximum of $|\tau_k - \alpha_k|$ is reduced to two cases:

$$\begin{aligned} \max_{\tau} \tau_k - \alpha_k &= \tau_k^U - \alpha_k, \\ \alpha_k - \min_{\tau} \tau_k &= \alpha_k - \tau_k^L. \end{aligned}$$

The first case requires condition $\alpha_k \leq \tau_k^U$. Condition $\alpha_k \geq \tau_k^L$ is for the second case. In sum, we get $C - 1$ linear programming problems (28) and $C - 1$ problems (29) with the same constraints (30)-(32) and different constraints (33). It is obvious that the final solution L of (27) is determined by comparison of all optimal terms $\alpha_k - \tau_k^U$ from (28) and optimal terms $\tau_k^L - \alpha_k$ from (29).

Proof of Proposition 3: The proof is similar to the proof of Proposition 2.

Proof of Corollary 4: Solutions (47) and (48) directly follows from the proof of Propositions 2-3 and from considering all variants of signs of $\pi_1 - \alpha_1$ and $\tau_1 - \alpha_1$.

Proof of Proposition 5: The lower bound is simply derived by introducing a new variable $B = \max_{i=1, \dots, C-1} |\pi_i - \alpha_i|$. The upper bound D^U can be derived similarly to problems (28)-(33) or (37)-(42). Let

$$k = \arg \max_i |\tau_i - \alpha_i|. \quad (66)$$

Introduce

$$D^U(k) = \max_{\pi, \alpha} |\pi_k - \alpha_k|.$$

Hence, we get two problems. The first one is

$$D_1^U(k) = \max_{\pi, \alpha} (\pi_k - \alpha_k),$$

subject to (30) and $\pi_k \geq \alpha_k$.

The second problem is

$$D_2^U(k) = \max_{\pi, \alpha} (\alpha_k - \pi_k),$$

subject to (30) and $\alpha_k \geq \pi_k$.

Solutions are trivial and have the form:

$$D^U(k) = \max \begin{cases} \pi_k^U - \alpha_k^L, & \text{if } \pi_k^U \geq \alpha_k^L, \\ \alpha_k^U - \pi_k^L, & \text{if } \pi_k^L < \alpha_k^U. \end{cases}$$

In sum, we get the upper bound as

$$D^U = \max_{k=1, \dots, C-1} D^U(k),$$

as was to be proved.

References

- [1] K. Aas, M. Jullum, and A. Loland. Explaining individual predictions when features are dependent: More accurate approximations to Shapley values. arXiv:1903.10464, Mar 2019.
- [2] J. Abellan, R.M. Baker, F.P.A. Coolen, R.J. Crossman, and A.R. Masegosa. Classification with decision trees from a nonparametric predictive inference perspective. *Computational Statistics and Data Analysis*, 71:789–802, 2014.
- [3] J. Abellan, C.J. Mantas, and J.G. Castellano. A random forest approach using imprecise probabilities. *Knowledge-Based Systems*, 134:72–84, 2017.
- [4] J. Abellan, C.J. Mantas, J.G. Castellano, and S. Moral-Garcia. Increasing diversity in random forest learning algorithm via imprecise probabilities. *Expert Systems With Applications*, 97:228–243, 2018.
- [5] J. Abellan and S. Moral. Building classification trees using th building classification trees using the total uncertainty criterion. *International Journal of Intelligent Systems*, 18(12):1215–1225, 2003.
- [6] A. Adadi and M. Berrada. Peeking inside the black-box: A survey on explainable artificial intelligence (XAI). *IEEE Access*, 6:52138–52160, 2018.
- [7] R. Agarwal, N. Frosst, X. Zhang, R. Caruana, and G.E. Hinton. Neural additive models: Interpretable machine learning with neural nets. arXiv:2004.13912, April 2020.
- [8] L. Antwarg, R.M. Miller, B. Shapira, and L. Rokach. Explaining anomalies detected by autoencoders using SHAP. arXiv:1903.02407v2, June 2020.
- [9] A.B. Arrieta, N. Diaz-Rodriguez, J. Del Ser, A. Bennetot, S. Tabik, A. Barbado, S. Garcia, S. Gil-Lopez, D. Molina, R. Benjamins, R. Chatila, and F. Herrera. Explainable artificial intelligence (XAI): Concepts, taxonomies, opportunities and challenges toward responsible AI. arXiv:1910.10045, October 2019.
- [10] V. Belle and I. Papantonis. Principles and practice of explainable machine learning. arXiv:2009.11698, September 2020.
- [11] V. Van Belle, K. Pelckmans, S. Van Huffel, and J.A. Suykens. Support vector methods for survival analysis: a comparison between ranking and regression approaches. *Artificial intelligence in medicine*, 53(2):107–118, 2011.
- [12] J. Bento, P. Saleiro, A.F. Cruz, M.A.T. Figueiredo, and P. Bizarro. TimeSHAP: Explaining recurrent models through sequence perturbations. arXiv:2012.00073, November 2020.
- [13] P. Bonissone, J.M. Cadenas, M.C. Garrido, and R.A. Diaz-Valladares. A fuzzy random forest. *International Journal of Approximate Reasoning*, 51:729–747, 2010.

- [14] D. Bowen and L. Ungar. Generalized SHAP: Generating multiple types of explanations in machine learning. arXiv:2006.07155v2, June 2020.
- [15] D.V. Carvalho, E.M. Pereira, and J.S. Cardoso. Machine learning interpretability: A survey on methods and metrics. *Electronics*, 8(832):1–34, 2019.
- [16] C.-H. Chang, S. Tan, B. Lengerich, A. Goldenberg, and R. Caruana. How interpretable and trustworthy are gams? arXiv:2006.06466, June 2020.
- [17] I.C. Covert, S. Lundberg, and S.-I. Lee. Explaining by removing: A unified framework for model explanation. arXiv:2011.14878, November 2020.
- [18] I.C. Covert, S. Lundberg, and S.-I. Lee. Understanding global feature contributions with additive importance measures. arXiv:2004.00668v2, October 2020.
- [19] I. Csiszar. Information type measures of differences of probability distribution and indirect observations. *Studia Scientiarum Mathematicarum Hungarica*, 2(:299–318, 1967.
- [20] A. Das and P. Rad. Opportunities and challenges in explainable artificial intelligence (XAI): A survey. arXiv:2006.11371v2, June 2020.
- [21] G.V. den Broeck, A. Lykov, M. Schleich, and D. Suciuc. On the tractability of SHAP explanations. arXiv:2009.08634v2, January 2021.
- [22] S. Destercke and V. Antoine. Combining imprecise probability masses with maximal coherent subsets: Application to ensemble classification. In *Synergies of Soft Computing and Statistics for Intelligent Data Analysis*, pages 27–35. Springer, Berlin, Heidelberg, 2013.
- [23] S.S. Dragomir, V. Gluscevic, and C.E.M. Pearce. Approximations for the csiszar’s fdivergence via mid point inequalities. In *Inequality Theory and Applications*, pages 139–154. Nova Science Publishers Inc., Huntington, New York, 2001.
- [24] D. Faraggi and R. Simon. A neural network model for survival data. *Statistics in medicine*, 14(1):73–82, 1995.
- [25] C. Frye, D. de Mijolla, L. Cowton, M. Stanley, and I. Feige. Shapley-based explainability on the data manifold. arXiv:2006.01272, June 2020.
- [26] D. Garreau and D. Mardaoui. What does LIME really see in images? arXiv:2102.06307, February 2021.
- [27] D. Garreau and U. von Luxburg. Explaining the explainer: A first theoretical analysis of LIME. arXiv:2001.03447, January 2020.
- [28] D. Garreau and U. von Luxburg. Looking deeper into tabular LIME. arXiv:2008.11092, August 2020.

- [29] R. Guidotti, A. Monreale, S. Ruggieri, F. Turini, F. Giannotti, and D. Pedreschi. A survey of methods for explaining black box models. *ACM computing surveys*, 51(5):93, 2019.
- [30] T. Hastie and R. Tibshirani. *Generalized additive models*, volume 43. CRC press, 1990.
- [31] Q. Huang, M. Yamada, Y. Tian, D. Singh, D. Yin, and Y. Chang. GraphLIME: Local interpretable model explanations for graph neural networks. arXiv:2001.06216, January 2020.
- [32] N.A. Ibrahim, A. Kudus, I. Daud, and M.R. Abu Bakar. Decision tree for competing risks survival probability in breast cancer study. *International Journal Of Biological and Medical Research*, 3(1):25–29, 2008.
- [33] K.C. Jain and P. Chhabra. Bounds on nonsymmetric divergence measure in terms of other symmetric and nonsymmetric divergence measures. *International Scholarly Research Notices*, 2014(Article ID 820375):1–9, 2014.
- [34] N.L. Johnson and F. Leone. *Statistics and experimental design in engineering and the physical sciences*, volume 1. Wiley, New York, 1964.
- [35] A. Jung. Explainable empirical risk minimization. arXiv:2009.01492, September 2020.
- [36] J.L. Katzman, U. Shaham, A. Cloninger, J. Bates, T. Jiang, and Y. Kluger. Deepsurv: Personalized treatment recommender system using a Cox proportional hazards deep neural network. *BMC medical research methodology*, 18(24):1–12, 2018.
- [37] A.V. Konstantinov and L.V. Utkin. Interpretable machine learning with an ensemble of gradient boosting machines. arXiv:2010.07388, October 2020.
- [38] M.S. Kovalev and L.V. Utkin. A robust algorithm for explaining unreliable machine learning survival models using the Kolmogorov-Smirnov bounds. *Neural Networks*, 132:1–18, 2020.
- [39] M.S. Kovalev, L.V. Utkin, and E.M. Kasimov. SurvLIME: A method for explaining machine learning survival models. *Knowledge-Based Systems*, 203:106164, 2020.
- [40] S. Kullback and R.A. Leibler. On information and sufficiency. *Annals of Mathematical Statistics*, 22:9–86, 1951.
- [41] Y. Liang, S. Li, C. Yan, M. Li, and C. Jiang. Explaining the black-box model: A survey of local interpretation methods for deep neural networks. *Neurocomputing*, 419:168–182, 2021.
- [42] M. Lichman. UCI machine learning repository, 2013.
- [43] Y. Lou, R. Caruana, and J. Gehrke. Intelligible models for classification and regression. In *Proceedings of the 18th ACM SIGKDD International Conference on Knowledge Discovery and Data Mining*, pages 150–158. ACM, August 2012.

- [44] S.M. Lundberg and S.-I. Lee. A unified approach to interpreting model predictions. In *Advances in Neural Information Processing Systems*, pages 4765–4774, 2017.
- [45] S. Mangalathu, S.-H. Hwang, and J.-S. Jeon. Failure mode and effects analysis of RC members based on machinelearning-based SHapley Additive exPlanations (SHAP) approach. *Engineering Structures*, 219:110927 (1–10), 2020.
- [46] C.J. Mantas and J. Abellan. Analysis and extension of decision trees based on imprecise probabilities: Application on noisy data. *Expert Systems with Applications*, 41(5):2514–2525, 2014.
- [47] R. Marcinkevics and J.E. Vogt. Interpretability and explainability: A machine learning zoo mini-tour. arXiv:2012.01805, December 2020.
- [48] P.-A. Matt. Uses and computation of imprecise probabilities from statistical data and expert arguments. *International Journal of Approximate Reasoning*, 81:63–86, 2017.
- [49] C. Molnar. *Interpretable Machine Learning: A Guide for Making Black Box Models Explainable*. Published online, <https://christophm.github.io/interpretable-ml-book/>, 2019.
- [50] I. Montes, E. Miranda, and S. Destercke. Unifying neighbourhood and distortion models: part ii – new models and synthesis. *International Journal of General Systems*, 49(6):636–674, 2020.
- [51] S. Moral. Learning with imprecise probabilities as model selection and averaging. *International Journal of Approximate Reasoning*, 109:111–124, 2019.
- [52] S. Moral-Garcia, C.J. Mantas, J.G. Castellano, M.D. Benitez, and J. Abellan. Bagging of credal decision trees for imprecise classification. *Expert Systems with Applications*, 141(Article 112944):1–9, 2020.
- [53] F. Nielsen and R. Nock. On the chi square and higher-order chi distances for approximating f-divergences. *IEEE Signal Processing Letters*, 21(1):10–13, 2014.
- [54] H. Nori, S. Jenkins, P. Koch, and R. Caruana. InterpretML: A unified framework for machine learning interpretability. arXiv:1909.09223, September 2019.
- [55] S. Onn and I. Weissman. Generating uniform random vectors over a simplex with implications to the volume of a certain polytope and to multivariate extremes. *Annals of Operations Research*, 189:331–342, 2011.
- [56] K. Pearson. On the criterion that a given system of eviations from the probable in the case of correlated system of variables is such that it can be reasonable supposed to have arisen from random sampling. *Philosophical Magazine*, 50:157–172, 1900.
- [57] V. Petsiuk, A. Das, and K. Saenko. RISE: Randomized input sampling for explanation of black-box models. arXiv:1806.07421, June 2018.

- [58] J. Rabold, H. Deininger, M. Siebers, and U. Schmid. Enriching visual with verbal explanations for relational concepts: Combining LIME with Aleph. arXiv:1910.01837v1, October 2019.
- [59] A. Redelmeier, M. Jullum, and K. Aas. Explaining predictive models with mixed features using shapley values and conditional inference trees. In *Machine Learning and Knowledge Extraction. CD-MAKE 2020*, volume 12279 of *Lecture Notes in Computer Science*, pages 117–137, Cham, 2020. Springer.
- [60] M.T. Ribeiro, S. Singh, and C. Guestrin. “Why should I trust You?” Explaining the predictions of any classifier. arXiv:1602.04938v3, Aug 2016.
- [61] M.T. Ribeiro, S. Singh, and C. Guestrin. Anchors: High-precision model-agnostic explanations. In *AAAI Conference on Artificial Intelligence*, pages 1527–1535, 2018.
- [62] C.P. Robert. *The Bayesian Choice*. Springer, New York, 1994.
- [63] R. Rodriguez-Perez and J. Bajorath. Interpretation of machine learning models using shapley values: application to compound potency and multi-target activity predictions. *Journal of Computer-Aided Molecular Design*, 34:1013–1026, 2020.
- [64] B. Rozemberczki and R. Sarkar. The shapley value of classifiers in ensemble games. arXiv:2101.02153, January 2021.
- [65] R.Y. Rubinstein and D.P. Kroese. *Simulation and the Monte Carlo method, 2nd Edition*. Wiley, New Jersey, 2008.
- [66] R.Y. Rubinstein and B. Melamed. *Modern simulation and modeling*. Wiley, New York, 1998.
- [67] C. Rudin. Stop explaining black box machine learning models for high stakes decisions and use interpretable models instead. *Nature Machine Intelligence*, 1:206–215, 2019.
- [68] C. Rudin, C. Chen, Z. Chen, H. Huang, L. Semenova, and C. Zhong. Interpretable machine learning: Fundamental principles and 10 grand challenges. arXiv:2103.11251, March 2021.
- [69] R. Senge, S. Bosner, K. Dembczynski, J. Haasenritter, O. Hirsch, N. Donner-Banzhoff, and E. Hüllermeier. Reliable classification: Learning classifiers that distinguish aleatoric and epistemic uncertainty. *Information Sciences*, 255:16–29, 2014.
- [70] S.M. Shankaranarayana and D. Runje. ALIME: Autoencoder based approach for local interpretability. arXiv:1909.02437, Sep 2019.
- [71] L.S. Shapley. A value for n-person games. In *Contributions to the Theory of Games*, volume II of *Annals of Mathematics Studies 28*, pages 307–317. Princeton University Press, Princeton, 1953.

- [72] E. Strumbelj and I. Kononenko. An efficient explanation of individual classifications using game theory. *Journal of Machine Learning Research*, 11:1–18, 2010.
- [73] N. Takeishi. Shapley values of reconstruction errors of PCA for explaining anomaly detection. arXiv:1909.03495, September 2019.
- [74] I.J. Taneja and P. Kumar. Generalized non-symmetric divergence measures and inequalities. *Journal of Interdisciplinary Mathematics*, 9(3):581–599, 2006.
- [75] L.V. Utkin and A.V. Konstantinov. Ensembles of random SHAPs. arXiv:2103.03302, March 2021.
- [76] P. Walley. *Statistical Reasoning with Imprecise Probabilities*. Chapman and Hall, London, 1991.
- [77] P. Walley. Inferences from multinomial data: Learning about a bag of marbles. *Journal of the Royal Statistical Society, Series B*, 58:3–57, 1996. with discussion.
- [78] M.N. Wright, T. Dankowski, and A. Ziegler. Unbiased split variable selection for random survival forests using maximally selected rank statistics. *Statistics in Medicine*, 36(8):1272–1284, 2017.
- [79] N. Xie, G. Ras, M. van Gerven, and D. Doran. Explainable deep learning: A field guide for the uninitiated. arXiv:2004.14545, April 2020.
- [80] J. Yu, Z. Lin, J. Yang, X. Shen, X. Lu, and T.S. Huang. Generative image inpainting with contextual attention. In *Proceedings of the IEEE Conference on Computer Vision and Pattern Recognition*, pages 5505–5514, 2018.
- [81] H. Yuan, H. Yu, J. Wang, K. Li, and S. Ji. On explainability of graph neural networks via subgraph explorations. arXiv:2102.05152, February 2020.
- [82] E. Zablocki, H. Ben-Younes, P. Perez, and M. Cord. Explainability of vision-based autonomous driving systems: Review and challenges. arXiv:2101.05307, January 2021.
- [83] M.D. Zeiler and R. Fergus. Visualizing and understanding convolutional networks. In *ECCV 2014*, volume 8689 of *LNCS*, pages 818–833, Cham, 2014. Springer.
- [84] X. Zhang, S. Tan, P. Koch, Y. Lou, U. Chajewska, and R. Caruana. Axiomatic interpretability for multiclass additive models. In *In Proceedings of the 25th ACM SIGKDD International Conference on Knowledge Discovery & Data Mining*, pages 226–234. ACM, 2019.
- [85] Y. Zhang, P. Tino, A. Leonardis, and K. Tang. A survey on neural network interpretability. arXiv:2012.14261, December 2020.